Northward expansion of the southern-temperate podocarp forest during the Early Eocene Climatic Optimum: Palynological evidence from the NE Tibetan Plateau (China)

Faez Robin-Champigneul, Julia Gravendyck, Huasheng Huang, Amber Woutersen, David Pocknall, Niels Meijer, Guillaume Dupont-Nivet, Roy H.J. Erkens, C. Hoorn

Northward expansion of the southern-temperate podocarp forest during the Early Eocene Climatic Optimum: Palynological evidence from the NE Tibetan Plateau (China)

Faez Robin-Champigneul, Julia Gravendyck, Huasheng Huang, Amber Woutersen, David Pocknall, Niels Meijer, G. Dupont-Nivet, Roy H.J. Erkens, C. Hoorn

PII: S0034-6667(23)00083-0

DOI: https://doi.org/10.1016/j.revpalbo.2023.104914

Reference: PALBO 104914

To appear in: *Review of Palaeobotany and Palynology*

Received date: 21 February 2023

Revised date: 10 May 2023

Accepted date: 11 May 2023

Please cite this article as: F. Robin-Champigneul, J. Gravendyck, H. Huang, et al., Northward expansion of the southern-temperate podocarp forest during the Early Eocene Climatic Optimum: Palynological evidence from the NE Tibetan Plateau (China), *Review of Palaeobotany and Palynology* (2023), https://doi.org/10.1016/j.revpalbo.2023.104914

Northward expansion of the southern-temperate podocarp forest during the Early Eocene Climatic Optimum: Palynological evidence from the NE Tibetan Plateau (China)

Robin-Champigneul, Faez [a*]; Gravendyck, Julia [b,c]; Huang, Huasheng[d]; Woutersen, Amber [e]; Pocknall, David [f]; Meijer, Niels [g]; Dupont-Nivet, G. [h]; Erkens, Roy H. J. [a,i]; Hoorn, C. [e*]

[a] Maastricht University, Faculty of Science and Engineering, Maastricht Science Programme, P.O. Box 616, 6200 MD Maastricht, The Netherlands.

[b] Leibniz University Hannover. Institute for Geology, Callinstraße 30, 30167 Hannover, Germany.

[c] Rheinische Friedrich-Wilhelms-Universität Bonn, Nees Institut for Biodiversity of Plants, Meckenheimer Allee 170, 53115 Bonn, Germany.

[d] Department of Earth Sciences, University of Florence, Via G. La Pira 4, 50121 Florence, Italy

[e] University of Amsterdam, Institute for Biodiversity and Ecosystem Dynamics, Science Park 904, 1090 GE Amsterdam, The Netherlands

[f] 314 Singing Sumac Way, San Marcos, TX 78666, USA

[g] Senckenberg Biodiversity and Climate Research Centre (SBiK-F), Frankfurt am Main, Germany.

[h] University of Rennes, CNRS, Géosciences Rennes, UMR 6118, 35000 Rennes, France.

[i] Naturalis Biodiversity Center, P.O. Box 9517, 2300 RA Leiden, The Netherlands

*Corresponding authors:

Faez Robin-Champigneul

f.robin-champigneul@alumni.maastrichtuniversity.nl

Carina Hoorn

m.c.hoorn@uva.nl

Abstract

The debated vegetation response to climate change can be investigated through palynological fossil records from past extreme climate conditions. In this context, the early Eocene (53.3 to 41.2 million years ago (Ma)) is often referred to as a model for a greenhouse Earth. In the Xining Basin, situated on the North-eastern Tibetan Plateau (NETP), this time interval is represented by an extensive and well-dated sedimentary sequence of evaporites and red mudstones. Here we focus on the palynological record of the Early Eocene Climatic Optimum (EECO; 53.3 to 49.1 Ma) and study the fossil gymnosperm pollen composition in these sediments. In addition, we also investigate the nearest living relatives (NLR) or botanical affinity of these genera and the paleobiogeographic implications of their occurrence in the Eocene of the NETP. To reach our objective, we complemented transmitted light microscopy with laser scanning- and electron microscopy techniques, to produce high-resolution images, and illustrate the morphological variation within fossil and extant gymnosperm pollen. Furthermore, a morphometric analysis was carried out to investigate the infra- and intrageneric variation of these and related taxa. To place the data in context we produced paleobiogeographic maps for *Phyllocladidites* and for other Podocarpaceae, based on data from a global fossil pollen data base, and compare these with modern records from GBIF. We also assessed the climatic envelope of the NLR. Our analyses confirm the presence of *Phyllocladidites* (NLR *Phyllocladus,* Podocarpaceae) and *Podocarpidites* (NLR *Podocarpus*, Podocarpaceae) in the EECO deposits in the Xining Basin. In addition, a comparative study based on literature suggests that *Parcisporites* is likely a younger synonym of *Phyllocladidites*. Our findings further suggest that the *Phyllocladidites* specimens are derived from a lineage that was much more diverse than previously thought, and which had a much larger biogeographical distribution during the EECO than at present. Based on the climatic envelope of the NLR, we suggest that the paleoclimatic conditions in the Xining

Basin were warmer and more humid during the EECO. We conclude that phylloclade-type conifers typical of the southern-temperate podocarp forests, had a northward geographical expansion during the EECO, followed by extirpation.

Keywords: Hyperthermal, Podocarpaceae, *Phyllocladus*, Palaeobiogeography, Palaeoclimate, Morphometry

1. Introduction

To obtain a better understanding of the implications of climate warming for plant composition and distribution (Kelly & Goulden, 2008; Moran et al., 2022), it is important to learn from past greenhouse conditions (Huber et al., 2018; Inglis et al., 2020). In particular, changes in paleobiogeographic distribution and turnover associated with the Early Eocene Climatic Optimum (EECO), spanning 53.3 to 49.1 Ma (Westerhold et al., 2018), forms a good analogue for extreme future warming scenarios, when global mean surface temperatures were 10 to 16^{o}C warmer than pre-industrial (Burke et al., 2018; Inglis et al., 2020), and latitudinal temperature gradients were less pronounced (Cramwinckel et al., 2018), even during winter (Greenwood & Wing, 1995). Such rare extreme conditions disappeared after the EECO, that was followed by a gradual, long-term global cooling trend, leading up to the Eocene–Oligocene Transition (EOT; 33.9 Ma). During the EOT, permanent Antarctic ice sheets formed (Coxall et al., 2005; Miller et al., 1991), that turned the global climate into an icehouse state, while cooling continued until the Quaternary (Cramwinckel et al., 2018; Westerhold et al., 2018).

Despite its interest, the EECO remains understudied, especially in continental Asia where rich sedimentary records including sporomorphs (i.e. pollen and spores), proved a useful proxy to evaluate vegetation changes through time (Ejsmond et al., 2011). For example, Li et al. (2022) reported major vegetation changes during the Eocene hyperthermal events in the Fushun basin, in north-eastern China. These authors observed a marked increase in the abundance of gymnosperm pollen, and a decrease in angiosperm pollen when compared to background intervals between hyperthermal events. Such observations suggested different vegetation groups have an affinity for different climatic conditions (Li et al., 2022; Xie et al., 2022). Earlier studies in the sedimentary basins of the NETP reported the presence of

Pinaceae pollen, but also Podocarpaceae, the latter including *Podocarpidites*, *Phyllocladidites*, and *Parcisporites* (Horton et al., 2004; Ma et al., 2012; Wang & Chang, 1990; Zhang & Zhan, 1991). However, these records did not have good age-control, nor did they place their occurrences in a palaeobiogeographic context, hindering their potential in resolving pending questions on the climate optima.

The interaction between climatic change and vegetation has been especially well-documented in the fossil record of the Xining Basin (NETP), where a highly diverse and abundant xerophytic vegetation occurred throughout the Eocene, which declined during the EOT while the Pinaceae conifer pollen increased (Dupont-Nivet et al., 2008; Hoorn et al., 2012; Wen et al., 2014; Barbolini et al., 2020). However, until now, the fossil pollen record of the EECO remained unexplored in the Xining Basin. A recently reported sedimentary record and dating of the EECO in the Xining Basin (Meijer et al., 2022) allows us here to provide new insights into vegetation composition and changes during extreme global warming. The sporomorph record in the EECO sediments of the Xining Basin (Meijer et al., 2022) includes many gymnosperm pollen types, which are particularly distinct and recognisable by their sacci that can vary in size, texture, and proportions across species (e.g. Erdtman, 1957; Traverse, 2007). The occurrences of the Podocarpaceae, including *Phyllocladidites* (NLR *Phyllocladus*), in the EECO strata of the Xining Basin are remarkable, as their current biogeographic range extends across e.g. New Zealand, Tasmania and Malesia (Fig. 2; Table S1). In this study we investigate the morphology of the Podocarpaceae pollen that were found in the palynological assemblage of the Xining Basin with the aim to identify them at genus level. Furthermore, we explore palynological databases and assess the Xining Basin occurrences and the global palaeogeographic extent of *Phyllocladidites*, *Podocarpidites*, and *Parcisporites* during the Palaeocene–Eocene warm periods.

(Figure 1, Figure 2 go here)

2. Regional setting

2.1. Geographic and geological setting

The Tibetan Plateau (TP) is the most extensive and highest plateau in the world, stretching over 2.5 million km^2, with an average elevation of over 4,500 m (e.g. Su et al., 2019; Wen et al., 2014). The growth of the TP was driven by the continental collision between the Indian and Asian tectonic plates since the Palaeocene (e.g. Kapp & DeCelles, 2019), while the inland proto-Paratethys Sea retreated westwards from Central Asia (e.g. Kaya et al., 2019). A smaller proto-Tibetan Plateau probably already existed before the Eocene due to terranes accreted during the Mesozoic (e.g. Kapp & DeCelles, 2019; Spicer et al., 2021; Su et al., 2019). After the India-Asia collision, the TP expanded towards the north and south (Tapponnier et al, 2001; Wang et al., 2008; 2014a), yet the precise elevation and detailed topographic pattern of the TP through time remains debated (e.g. Botsyun et al., 2019; Spicer et al., 2021). The Xining Basin located in NE Tibet (Fig. 3), likely formed at lower elevation in a slowly subsiding extensional setting during the Cretaceous and Eocene (Horton et al., 2004; Yuan et al., 2013). Exhumation and the occurrence of conglomerates suggests that some topography already existed (Clark et al., 2010; Meijer et al., 2022), but most of the deformation occurred later during the Neogene resulting in segmented sub-basins separated by uplifting mountain ranges (Horton et al., 2004; Meijer et al., 2022). The Eocene sedimentary strata consist of the Qijiachuan and Honggou Formations which are both composed of mudrocks and evaporites deposited on a distal alluvial mudflat (e.g. Meijer et al., 2022). The provenance of pollen found in this setting has been interpreted as coming from local taxa of which the parent plant grew on the mudflats, but also from high-altitude tree

taxa that inhabited the peripheral mountains (Barbolini et al., 2020; Dupont-Nivet et al., 2008; Hoorn et al., 2012; Page et al., 2019).

(Figure 3 goes here)

2.2. Regional vegetation and the palaeobotanical record

The TP forms part of the Central Asian steppe-desert biome (CASDB), and the flora of this biome is dominated by xerophilous herbs including Poaceae, Chenopodioideae, and Asteraceae (Barbolini et al., 2020; Wesche, 2016). The slopes of mountain ranges, such as the Tianshan and Altai, typically host steppe vegetation in the basin and forest on the slopes, with the higher elevations primarily populated by Pinaceae (Barbolini et al., 2020). This botanical composition differs strongly from the vegetation in the middle to late Eocene, when the vegetation on the TP was characterised by high abundances of xerophytic steppe taxa consisting of shrubs such as Ephedraceae and Nitrariaceae (Barbolini et al., 2020; Hoorn et al., 2012; Woutersen et al., 2023), comprising as much as 80% of the pollen sum. For comparison, in Holocene records pollen percentages of the Ephedraceae are limited to c. 20% (Wang et al., 2022), while the Nitrariaceae are absent or rare. The remaining of the pollen sum was formed by temperate broad-leaved and conifer forest taxa from the peripheral mountain slopes (Barbolini et al., 2020; Bosboom et al., 2014; Hoorn et al., 2012).

2.3. Past and present records of conifers in Central, East- and Southeast Asia

Conifers were abundant in Central Asia during the Cretaceous and early Palaeogene, including Pinaceae and Podocarpaceae (Wang et al., 1990; Zhang & Zhan, 1991). However, in the Eocene sediments of the Xining Basin, conifer pollen are rare and only (re)appear at ca. 37 Ma, with high altitude Pinaceae forming an important component of the regional flora

(Barbolini et al., 2020; Dupont-Nivet et al., 2008; Hoorn et al., 2012; Page et al., 2019). The Pinaceae are a broad lineage that originated in Laurasia in the Early Jurassic, following the continent's separation from Gondwana, and since their diversification are primarily distributed in the northern hemisphere (Gernandt et al., 2008; Gernandt et al., 2018; Leslie et al., 2012). They are widely reported in Asia, including in the Xining Basin where they occur in Cretaceous and Eocene sediments (Dupont-Nivet et al., 2008; Hoorn et al., 2012; Wang et al., 1990; Zhang & Zhan, 1991). Nowadays, although distributed across the northern hemisphere, they are particularly highly concentrated in North America and southern China (Leslie et al., 2012). The shift to Pinaceae dominance at the EOT (ca. 34 Ma) is likely a response to cooling temperatures and higher seasonal aridity, which are tied to global cooling and the retreat of the proto-Paratethys Sea (Barbolini et al., 2020; Han et al., 2016; Hoorn et al., 2012).

The Podocarpaceae, a primarily southern-hemisphere lineage, originated in Gondwana and include extant genera such as *Podocarpus* and *Phyllocladus* (Morley, 2011). *Podocarpidites* (fossil *Podocarpus* pollen) is recognisable by large fan-like sacci, and *Phyllocladidites* (fossil *Phyllocladus* pollen) by its diminutive sacci (Cookson, 1947; Couper, 1953). The latter is thought to have diverged early from other Podocarpaceae and has such distinctly different pollen morphology that some argue should be classified in its own family, the Phyllocladaceae (Keng, 1973, 1978; Molloy & Markham, 1999; Page, 1990; Tomlinson et al., 1997; Wagstaff, 2004; see Fig. 1 for features of *Phyllocladus*). The modern *Podocarpus* species have a far broader range than *Phyllocladus*, with records in Central and South America, Sub-Saharan Africa, East- and Southeast Asia, and Australia (Fig. 2; GBIF.org, 2022a). Meanwhile, the range of modern *Phyllocladus* is more restricted, with records in

New Zealand, Tasmania, Malaysia, Borneo, Sulawesi, New Guinea, and the Philippines (Fig. 2; GBIF.org, 2022b; Korasidis et al., 2019; Mildenhall, 1980; Morley, 2011; Pocknall, 1981). The biogeographic range of *Phyllocladus* overlaps with *Podocarpus* in Southeast Asia and Australasia (Fig. 2), where they co-occur as mixed podocarp forests. The overlap in range between the two genera is characterised by mean annual temperatures ranging from 6.9°C (New Zealand) to 25°C (Maluku and New Guinea) and mean annual precipitation from 1,438 mm/year (Tasmania and Australia) to 3,148 mm/year (New Guinea), with minimal annual temperatures from -2.6°C (New Zealand) to 21°C (Maluku and New Guinea) (Table S5 in Biffin et al, 2012). There are also a small number of dispersed records in North America and in Europe. However, explaining their low density and distance to the regular range of *Podocarpus* and *Phyllocladus*, we find that these are records belonging to museum or botanical garden specimens (GBIF.org, 2022a, 2022b).

3. Materials and Methods

3.1 Samples and age model

The organic residue studied was obtained from sedimentary rocks from the following sections within the Xining Basin (Fig. 3; Meijer et al., 2022): Bingling Shan (36° 27′ 13″ N, 101° 58′ 51″ E), Caija (36° 36′ 55″ N, 101° 58′ 03″ E), East Xining (36° 34′ 50″ N, 101° 53′ 42″ E), and Xiejia (36° 31′ 20″ N, 101° 52′ 20″ E). Ages of the samples are derived from a Bayesian age-depth model (Fig. S1; Haslett & Parnell, 2008; Trayler et al., 2019) using the preferred magnetostratigraphic correlation in Meijer et al. (2022) with the astronomically tuned geomagnetic polarity timescale of Gradstein et al. (2020). The studied samples range from 53.0 to 43.4 Ma (Table 1).

(Table 1 goes here)

3.2 Palynology

3.2.1. Preparation and Imaging

Samples from Bingling Shan, Caijia, and Xiejia were processed by Palynological Laboratory Services in Anglesey, UK, applying standard palynological procedures using freeze drying, acid treatment with 20% hydrochloric acid (HCl) and 40% hydrofluoric acid (HF), a 10 µm sieve, and drying at <50 °C. Samples from East Xining were processed at the Institute for Biodiversity and Ecosystem Dynamics (IBED), University of Amsterdam. The organic residue was mounted on microscope slides using Kaiser's glycerine gelatine and sealed with paraffin. The methodology is further detailed in Huang et al. (2020). Additional material from East Xining was mounted in fluorescent neutral Entellan®Neu (Merck) at the Leibniz University Hannover to facilitate both light and fluorescent light imaging techniques. Herbarium material was selected for comparison of the fossil sporomorphs with candidate Nearest Living Relatives. We compared the fossil Podocarpaceae pollen to modern Podocarpaceae pollen samples, which were on loan from Naturalis Biodiversity Center (Leiden, The Netherlands; see Table 2).

(Table 2 goes here)

Imaging was performed using a Leica DM700 light microscope (LM) mounted with a Leica ICC50 HD camera (magnification 0.5x). Slides were screened at 20x magnification for relevant specimens, which were documented through a 63x water objective, and processed using the Leica Application Suite X software (LAS X, Leica Microsystems). A total of 318 fossil specimens and 41 modern specimens were imaged. The locations of each specimen are recorded with England Finder (EF) references. Selected specimens were additionally documented with a TCS SP8 STED confocal microscope (Leica Microsystems, Wetzlar,

Germany). Images were produced using a 63x oil objective and a white light laser set to 561 nm.

Additional examinations were made on an Olympus BX53 mounted with an 100x oil objective and Olympus XC50 Camera. Selected specimens were imaged with an LSM 980 Airyscan (Carl Zeiss, Jena, Germany). This is a state-of-the-art laser scanning imaging technique with 32 detectors instead of one photomultiplier detector used in standard confocal methods (Huff, 2015; Huff et al., 2019; Romero et al., 2020b; Sivaguru et al., 2018). Images were acquired with a 60x oil objective, 3 lasers (405, 488 and 561 nm), scan speed 7, unidirectional scan repeating per line with 8x averaging, and slice thickness of 0.13 µm. Depicted images were processed with super resolution function and deconvolution at good medium speed. Extended depth of focus was achieved with maximum projection.
Finally, SEM images were produced to capture the surface texture of pollen grains in high resolution. Samples were strew mounted on cover slips, dried on a heat plate, and sputter coated with 4nm Palladium. These were then imaged using a TESCAN CLARA.
The photographs are provided in Plates I-VII, and in Supplementary Plates A & B.

3.2.2. Sporomorph composition

The sporomorph composition of three representative samples from the East Xining section was established. The analysed samples were PEX 12-08 (P12), PEX 15-08 (P15) and PEX 17-08 (P17), ranging in age from 53.02 (52.81-53.52) to 52.36 (52.11-52.57) Ma (Meijer et al., 2022). In total, 857 sporomorphs were counted in the corresponding microscope slides and grouped into ecological groups following Hoorn et al. (2012). The original count did not discriminate much between bisaccate types, so an additional count was performed based on earlier imaging work, covering 53 specimens over the three samples, from which ratios were

calculated and combined with the data from the primary count, including non-bisaccate Pinaceae (*Tsugaepollenites* and *Laricoidites*), to produce an estimation of the Pinaceae-Podocarpaceae ratio of conifer types. The count data is presented in Table S2, with percentages represented in a pie chart (Fig. 4).

3.2.3. Morphometric analysis

Measurements were taken in ImageJ Fiji (Rueden et al., 2017; Schindelin et al., 2012) based on the defining characteristics of bisaccate pollen documented in Traverse (2007; cf. Fig. 5). This data was then subjected to a PCA analysis to identify clusters based on the measurements rather than visual observation alone. Measurements of modern pollen were included in the PCA as markers to help identify the nature of the clusters. A total of 111 fossil and 41 modern specimens were measured. Polar view was the most widespread orientation, accounting for 89 fossil specimens and 40 modern specimens. Due to constraints in R, the final PCA contains only grains in polar orientation for which all seven measurements were available, i.e. excluding degraded grains. This resulted in a dataset of 63 fossil and 40 modern pollen specimens (*Phyllocladus hypophyllus* (10), *Phyllocladus trichomanoides* (10), and *Podocarpus macrophyllus* (20)) being subjected to PCA analysis. The PCA analysis was performed in RStudio version 1.4.1717 (RStudio Team, 2021), running R version 4.1.1 (R Core Team, 2021) using the default statistics package, ggplot2, and pca3d (R Core Team, 2021; Weiner, 2020; Wickham, 2016).

Clusters were identified based on their proximity to modern taxa and were further resolved based on morphological characteristics not included in the PCA analysis, such as saccus texture and shape, using as primary reference the original descriptions (Cookson, 1947;

Couper, 1953). Chinese reference literature was used to further refine our results (namely Song et al., 1985, 1999; and Zhang & Zhan, 1991), which includes pollen descriptions from the Cretaceous and Cenozoic in China, thus including the types we expect to find in the EECO samples.

3.3. Biogeographical analysis

To study the biogeographic changes of the Podocarpaceae over the Cenozoic, our data was compared to that of other palynological records. First, modern distribution data was downloaded from GBIF for both *Podocarpus* and *Phyllocladus*, restricting data as per Woutersen et al. (2018) to records with coordinates, and for which the basis of record was listed as 'Observation-only', 'Human observation', and 'Preserved specimen'. Exported occurrence data was cleaned with the software package CoordinateCleaner (Zizka et al., 2019) to exclude misplaced occurrence points. Climate data covering six variables (mean annual temperature, maximum temperature of warmest month, minimum temperature of coldest month, annual precipitation, precipitation of wettest month, and precipitation of driest month) for both *Podocarpus* and *Phyllocladus* was extracted from the WorldClim Version 2 (https://worldclim.org/version2, 30s in resolution) for the grid-based cleaned-GBIF data, which was used to understand the drivers of the distribution shift of the studied taxa in their biogeographical histories. As a supplement for discussion, MAT data was also referred to the PALAEOFLORA database (http://www.palaeoflora.de): 5.8–26.8 °C for *Phyllocladus sp*., 12.9–26.9 °C for *Podocarpus macrophyllus*, and 4.9–27.7 °C for *Podocarpus sp*.

To collect palaeobiogeographic data, we followed the methodology laid out in Lim et al. (2022). Palaeocene and Eocene records of *Phyllocladidites* and *Phyllocladus* (which was corrected to the accepted palynological name *Phyllocladidites* during analysis) were first obtained from the Palynodata database (Palynodata Inc. & White, 2008). We additionally

included records of *Parcisporites* in the dataset, due to the remarkable overlap in morphology between the taxa, which we elaborate further in this paper. *Parcisporites* corresponds to what we label as *Phyllocladidites* in the Chinese palynological literature, including literature relating to our area of interest (e.g. Zhang & Zhan, 1991).

The reports were all checked and sorted into three levels of confidence: 1) low, for untraceable or inaccessible literature; 2) medium, for traceable literature but for which the identification of the palynomorphs could not be assessed (e.g. without pollen micrographs); and 3) high, for literature for which we could assess the identification using provided micrographs. As Palynodata only includes literature until 2006, we used Google Scholar to augment the record with more recent reports as suggested by Gravendyck et al. (2022a, b). Palaeomaps on the Palaeocene and Eocene were then constructed with medium- and high-confidence occurrence data, and the Advanced Plate Tectonic Reconstruction Service from the ODSN (https://www.odsn.de/odsn/services/paleomap/adv_map.html) using an Equidistant Cyclindrical projection. A stratigraphic chart for visualising the ranges of each form-species within *Phyllocladidites* and *Parcisporites* was also created according to biogeographical realms.

4. Results

4.1. General comments

The Tibetan assemblages are well preserved and sporomorphs are abundant, especially in samples from East Xining. As shown in Figure 4, the steppe-desert biome is by far the best represented in the sporomorph assemblage, and mainly formed by Ephedraceae (Gnetales). Temperate forests are fairly represented, with traces of both broadleaf and coniferous forests. In the latter, we find primarily bisaccate pollen consisting of Pinaceae (*Piceapollenites*,

Tsugaepollenites, *Pinuspollenites*, etc.) and Podocarpaceae (*Podocarpidites* and *Phyllocladidites*), with a ratio of roughly 64:36. Spores are very rare. A more detailed palynological analysis of the assemblage is beyond the scope of this paper and will be presented in a separate study. The colour and preservation of specimens is mostly uniform, although some specimens of Ephedraceae (gymnosperms) and Nitrariaceae (angiosperms) showed infraspecific colour variation.

(Figure 4 goes here)

4.2. Systematic Palynology

Phyllocladidites Cookson 1947 ex Couper 1953 emend.

Type Species: *Phyllocladidites mawsonii* Cookson ex Couper 1953

1947 Cookson, p. 133, Pl. 14, figs 22-28.

Plates I-V, & VII

Original Diagnosis: Grains of medium size, with two small air bladders, which, when expanded, do not extend far beyond the equator of the grain; body of grain ellipsoidal, with a wide clearly defined furrow. The exine is firm, finely granular and conspicuously thickened at the proximal root of each bladder. (Cookson, 1947, p. 133)

*Description***:** Small to medium bisaccate palynomorphs with a circular to oval corpus, the dimensions of which generally represent the overall dimensions of the pollen grain in polar view. Their main distinguishing feature is a pair of diminutive sacci on either side of the grain, aligning either with the major or minor axis (Plate I). The exact morphology is highly variable and three types (1-3) can be tentatively differentiated based on the size and thickness of the sacci (see comparison below). Overall, pollen size varies within each type and between

types (e.g. Plate I, 3 compared to Plate I, 17). Note that this effect can be elevated by different embedding media, i.e. smaller specimens were documented from Entellan in comparison to specimens from glycerine-jelly (Plate I, 11, 27 and 28). Apart from overall size, saccus morphology is the most variable feature. Sacci can be almost absent (Plate I, 1 and 6), rather short (e.g. Plate I, 3, 8, 11, Plate II, Plate VII, 1) to almost encircling the grain (e.g. Plate I, 25, 27, 28) with intermediate forms of partially merged sacci (e.g. Plate I, 12, 13, 16-19, 25-28, Plate III). The saccus itself can be straight (e.g. Plate I, 7) or folded (e.g. Plate I, 23, 27, also in extant *Phyllocladidites trichomanoides*, Plate I, 29), but they are always very thin relative to the overall grain size.

Some specimens summarised as **Type 1** have a thin wall and small sacci and bleach easily when observed with lasers (Plate I, 8, 13, 19, 22, Plate II, 2, 3). Specimens of **Type 3** show the opposite trend with thick wall and almost no bleaching despite the same laser and scanning settings (Plate IV, 2, 3). The saccus size is also variable; small, diminutive sacci that barely extend from the corpus are typical of Type 1 (Plate I), and sacci that extend past the corpus are typical of **Type 2** (Plate I, Plate V) and are comparable to those in extant *Phyllocladidites trichomanoides* (Plate I, 29). Saccus morphology is not only variable in between specimens but often variable on the same grain with one saccus usually being smaller and/or more folded than the other (Plate I, 4, 10, 11, 20, 30, typical of Type 3).

Dimensions: See Table 3.

Occurrence: These types occur in the Xining Basin in samples P12, P15, P17, and NB6, therefore between 53.02 and 52.38 Ma. They were not found in the younger samples.

Remarks: The conspicuously smaller sacci are characteristic of *Phyllocladidites* and are also the only discriminating characteristic of the two-year younger genus *Parcisporites* (Leschik, 1955) whose diagnosis reads: *"Development of the sacci incomplete. Mostly two small wings; these partially distributed along the zona with an irregular outline."* (translated from German after Leschick, 1955, p. 55). Leschik describes four new species under his new genus. The type for the genus *Parcisporites annectus* is also described as granular and possessing a furrow, both features are also mentioned in the circumscription of *Phyllocladidites*. All in all, the newly described taxa from Leschik could have been accommodated under *Phyllocladidites* Cookson ex Couper.

Although citing both Cookson and Couper's publications, Leschik neither compared to or distinguished *Parcisporites* from *Phyllocladidites*. In fact, Leschik only provides descriptions, but no distinguishing characteristics, i.e., a diagnosis in the nomenclatural sense. Unfortunately, the holotype material for Leschik is unavailable for study. An attempt to uncover the material in 2018 by JC has been unsuccessful and the material is presumed to be lost. Based on the only remaining evidence, i.e., the protologue the later erected genus *Parcisporites* appears superfluous.

Many taxa, that could have been probably better accommodated under *Phyllocladidites* were described under *Parcisporites* from China and compare relatively well with the herein described forms. Zhang & Zhan (1991; p.173–175) reported four new species:

(1) *Parcisporites antiquus* Zhang et Zhan, which has only slightly bigger/more inflated sacci than *Parcisporites parvisaccus* Song et Zheng and which might represent forms that we included in Type 3 with distinct sacci on either side (Plate II, 15, 21), juxtaposed with those

thinner-walled forms of Type 1 (Plate II, 2, 7, 11) which might be more comparable to Song and Zheng's *Parcisporites parvisaccus*;

(2) *Parcisporites tarimensis* Zhang et Zhan, which we consider a variant of *Parcisporites apertus;*

(3) *Parcisporites apertus* Zhang et Zhan, which looks very comparable to *Parcisporites. annulatus* Wang and some of our specimens with merged sacci (Plate II, 17, 25, 22, 27, 28);

(4) *Parcisporites bellus* Zhang et Zhan, with an additional central saccus, has no equivalent in our material. The other forms reported by Zhang and Zhan (1991) are however comparable to our observed variation. For example, *Parcisporites auriculatus* Song et Cao resembles a specimen from Type 2 (Plate II, 20) and *Parcisporites fushunensis* Song et Cao looks like our specimen from Plate V.

Podocarpidites Cookson 1947 ex Couper 1953

Type Species: *Podocarpidites ellipticus* Cookson ex Couper 1953

1947 Cookson, pp. 131-132, Pl.13, figs 5-7.

Plate VI & VII

Original Diagnosis: This sporotype is proposed for fossil pollen grains with two air bladders of the type met with in *Podocarpus* when it is not known whether they have been derived from either *Podocarpus, Dacrydium* or some extinct member of the Podocarpaceae.

Description: *Podocarpidites* is distinguishable by its relatively large sacci, that are often wider than the central body (Plate VI, 1, 2; Plate VII, 7). The sacci typically attach to a significant part if not all the periphery of the central body are roughly fan-shaped and have a fine reticulum (Plate VI, 3). Ornamentation on the corpus varies from granulose (e.g.

Podocarpidites wapellensis Pocock 1970) to highly sculptured/rugulate (e.g. *Podocarpidites rugulatus*; Plate VI, 4, Plate VII, 7).

Dimensions: See Table 3.

Occurrence: These types occur in the Xining Basin in samples P12, P15, P17, and NB6, therefore between 53.02 and 52.38 Ma, and were not found in younger samples.

Remarks: Distinctly rugulate forms can be distinguished either on species level (e.g., *Podocarpidites rugulatus* Pocknall et Mildenhall 1984) or on genus level (*Rugubivesiculites* Pierce 1961). The genus level designation is more commonly used for Cretaceous fossils (Falcon-Lang et al., 2003), but some use it also in the Cenozoic specimens (Berry, 2022; Chen et al., 2019). The overall size of the pollen varies but they retain distinctive common shapes and proportions.

(Tables 3 and Plates I-VII go here)

4.3. Morphometry

There is little apparent clustering other than possible broad groups in the produced plot, even though the PCA axes account for a total of 81.03% of the variance between types (Fig. 5). To see whether any important information was missing from the two-dimensional PCA, we also plotted the results in three dimensions, which shows that when plotted together, the overall clustering is roughly identical (Fig. S2). This suggests that bisaccate pollen types can be quite difficult to accurately distinguish, as there is significant overlap in morphology and dimensions between bisaccate pollen. Formal descriptions of bisaccate gymnosperm palynomorphs are rarely mutually exclusive (e.g., see Jansonius & Hills, 1976). Many

micrographs and additional descriptions in Song et al. (1985), Song et al. (1999), and Zhang & Zhan (1991) were used to refine our results. The modern *Podocarpus* and *Phyllocladus* pollen also helped to highlight where the fossil Podocarpaceae are positioned in the PCA chart. Whilst the modern *Phyllocladus hypophyllus* and *P. trichomanoides* cluster closely together and form a distinct group within the graph, fossil *Phyllocladidites* is sufficiently distinct and arguably does not require the modern pollen markers to define a cluster. We note that different groups of fossil taxa tend to cluster along PC2 (30.86%) whilst occupying a large range on PC1. This suggests that whilst saccus morphology, especially distance between sacci and saccus height, is very important in distinguishing types, the total width is the least relevant. This largely concurs with our discussion in section 4.2. The modern and fossil *Phyllocladus*-type pollen form a rough 'layer' at the top of the graph. Similarly, the *Podocarpidites* form a layer at the bottom of the graph, and the presence of the modern *Podocarpus macrophyllus* dispersed in this layer would suggest our identification to be largely correct, although the margins of the *Podocarpidites* layer are far less distinct. Note however that the boundary between *Podocarpidites* and Pinaceae pollen is less clear due to morphological similarities.

(Figure 5 goes here)

4.4. Palaeobiogeography and palaeoclimate

Once filtered, we obtained 44,585 modern occurrences of *Podocarpus* and 19,148 of *Phyllocladus*. Based on palaeobiogeographical data, there were 29 high- and 40 medium-confidence reports in the Eocene, and 8 high- and 13 medium-confidence reports for the Palaeocene (Figures 6, 7; Tables S3 and S4). Low-confidence records in the Palaeocene (40) and Eocene (57) were excluded from the map. However, we note that our sampling location lies outside the range of modern *Podocarpus*, and far out of the range of modern

Phyllocladus by several thousands of km (nearest occurrence at 2,891 km), but within the palaeogeographic range of *Phyllocladidites*. In the Eocene, the palaeogeographic extent of *Phyllocladidites* was much broader than at present, extending from Antarctica and South America to Central Asia. The geographical extent of the Palaeocene record is like that of the Eocene, but the data is sparser.

Extracted climatic envelopes for the six climate variables suggest that *Podocarpus* has a broader niche than *Phyllocladus* (Fig. 8; Table S5), which can account for the differences between their distribution ranges (cf. Fig. 2). Furthermore, compared with *Phyllocladus*, *Podocarpus* preferably grows in a warmer and more arid habitat (Fig. 8). Nevertheless, both genera favour warm and humid settings with a MAT of ca. > 10 °C (75%), and a MAP of > 1000 mm (75%) (Fig. 8). The MAT values (5.3–26.6 °C for *Phyllocladus sp*., 12.9–26.9 °C for *Podocarpus macrophyllus*, and 4.9–27.7 °C for *Podocarpus sp*.) from the PALAEOFLORA database (http://www.palaeoflora.de) also indicate their thermophilous character.

(Figure 6, Figure 7, and Figure 8 go here)

In the samples from the Xining Basin, the presence of gymnosperm pollen is observed in samples of 52.4 Ma and older, with *Podocarpidites* and *Phyllocladidites* only found at or before 52.4 Ma. The disappearance of the podocarps and other bisaccate pollen from our samples very roughly coincides with the decline of the EECO, ending around 49 Ma (Westerhold et al., 2018).

4.5. Limitations

A limitation of this study —and the pollen record in general— was the difficulty in accurately distinguishing between pollen types, even with a morphometric analysis (e.g.

Bogotá-Ángel et al., 2021). This is especially true with regards to *Podocarpidites*, *Podocarpus*, and Pinaceae. However, this could be resolved by having a more comprehensive morphometric analysis, including traits such as the texture of the sacs and corpus, exine thickness at the equator, or angles of sac attachment, which were not quantified in this study. Furthermore, additional measurements of other modern pollen from more taxa could be used to create more points of reference in the PCA plot. Additionally, we could reduce bias by employing machine deep learning, especially in combination with super-resolution imaging (Romero et al., 2020a), and complementing the morphological data with chemical data, see for example Woutersen et al. (2018).

We also considered the possibility of reworking from older sediments. We observed variation in colour in some angiosperm pollen of the same taxon, however, not in the pollen that were the subject of this study. Although a darker colour alone is normally interpreted as a result of thermal maturation (Goodhue & Clayton, 2010; Staplin, 1969), the combined occurrence of darker and non-dark taxa (especially in the same taxon) can indicate reworking (Traverse, 2007). Nevertheless, there are several environmental factors during deposition that are hypothesised to also create such colour variation (e.g. acidification) (e.g. Pieńkowski et al., 2012; van de Schootbrugge et al., 2009). Another tentative sign of reworking could be a single find of a *Eucommiidites* grain in PEX 15-08, a taxon that ranges from the Triassic to Cretaceous, but also the presence of *Classopollis* in PEX 15-08. Given the abundance and perfect preservation of palynomorphs in the studied material, singular occurrences of these poorly preserved grains are, however, only weak palynological evidence of possible reworking.

5. Discussion

5.1. Taxonomy and nomenclature

The genus *Phyllocladidites* has previously been considered as an extinct taxon belonging to the Podocarpaceae, with a preference for tropical to sub-tropical temperate and humid environments (Cui et al., 2015; Schrank, 2010; Wang et al., 2014b). *Phyllocladidites* was first described from the Palaeogene of Australasia and is characterised by small sacci that do not extend beyond the corpus (Cookson, 1947; Couper, 1953). The same minute sacci are considered indicative of *Parcisporites* which was first described from the Triassic of Switzerland (Leschik, 1955). Based on the circumscription of the two taxa they seem indistinguishable.

According to citations referenced in Palynodata (Palynodata Inc. & White, 2008; Gravendyck et al., 2022a, b), 31 species of *Parcisporites* have been described; 8 from Triassic sediments and 23 from Cretaceous to the Palaeogene rocks exclusively from China by Chinese authors. *Phyllocladidites* not only has more overall references (396 in contrast to 114 for *Parcisporites*), but also has Chinese as well as non-Chinese references and a worldwide distribution. Nevertheless, most references (ca. 70%) for the Palaeogene are from Australasia. This difference in name usage poses the question whether it encodes a biological or rather a metaphysical signal, e.g. the conventions of different palynological schools or conventional use of names in specific time intervals.

In literature, *Phyllocladidites* and *Parcisporites* are rarely mentioned together with an exception in Li et al. (2019) who identified *Parcisporites* and specifically commented on the absence of *Phyllocladidites*. Song et al. (1999) suggested that *Phyllocladidites inchoatus* and *Parcisporites minutus* should be considered synonymous. The otherwise very rare use or commentary on *Phyllocladidites* in Chinese literature suggests that this is simply a

conventional, rather than a biological cause. Such separation of taxa based on different languages, geography or palynological schools has been exemplified for other taxa before (Gravendyck, 2021; Gravendyck et al., 2022b; Gravendyck et al. 2023) and might also explain the disjunct use of *Parcisporites* and *Phyllocladidites.*

Comparing some species described for *Parcisporites* (e.g., Wang & Chang (1990; 8 species), and Zhang & Zhan (1991; 4 species)) with our observed morphological variation, there is a large morphological overlap between the described forms of *Parcisporites* with the herein observed diversity (see systematic palynology section for details). It should be noted that the often-poor visual documentation and hard to understand circumscriptions make final judgement as to potential synonyms or distinctions of different species difficult. In general, the immense diversity of forms and inconsistency of morphologies (especially the saccus) seems to be the most consistent character of *Phyllocladidites/Parcisporites.* This is exemplified in Types 1-3 described in this paper.

The protologues for both *Phyllocladidites* and *Parcisporites* are described rather broadly. The circumscription of the latter can be accommodated under the former. Unfortunately, there is little to no possibility to reinvestigate the presumably lost holotype material. If not considering the two taxa as heterotypic synonyms, then *Phyllocladidites* should take priority. Even if not considering the two taxa synonymous, the poorly defined and thus ambiguous name *Parcisporites* should at least be limited to the type to avoid future taxonomic confusion, which is common practice for example when revising dinoflagellate taxonomy (Fensome et al., 2019).

5.2. Morphometry

In our study we noted considerable size variation not only between mounting media but also within species. Most specimens of *Phyllocladidites* are larger than *Phyllocladus* (Fig. 5). Some of the size differences are the result of swelling due to the glycerine jelly mounting medium. This phenomenon has been well documented (e.g. Praglowski, 1970; Sluyter, 1997; Wei et al., 2023) with significant swelling occurring in the first 3 years of storage. Apart from the secondary preparation effect, the observed size variation might be a biological signal as it was observed also in material of the same type of preparation.

One influencing factor of pollen size variation might be varying ploidy levels in different parent plant individuals or populations. Although not always a consistent measure, ploidy levels in some taxa have been shown to correlate with pollen size (Altmann et al., 1994; De Storme et al., 2013; Srisuwan et al., 2019). Variation in ploidy can come in many forms like polyploidy (duplication of chromosome sets), aneuploidy or dysploidy (gain or loss of single chromosomes) (de Wet, 1971; Escudero et al., 2014). Modern Podocarpaceae are known to exhibit dysploidy, and additionally have wide differences in monoploid karyotypes within the genera *Dacrydium* and *Podocarpus* (Khoshoo, 1961). Although modern *Phyllocladus* have a karyotype of n = 9, modern taxa are also very closely related, unlike its fossil counterparts, which may have been far more diverse (Khoshoo, 1961; Wagstaff, 2004). Therefore, it is possible that strongly varying pollen sizes observed in *Phyllocladidites* and *Podocarpidites* pollen material might attest to different palaeoploidy levels in the observed taxa. The fact that dysploidy generally persists longer over time than polyploidy (Escudero et al., 2014), in combination with present day dysploidy in the few remaining podocarps might further support this interpretation.

Alternatively, the highly variable overall morphology (i.e. saccus variations in size and morphology, overall size) could also be the result of natural variation which can be higher in some taxa as opposed to others and can be shaped and selected for to maximise adaptation to different reproductive strategies, environments, or pollination success (Fatmi et al., 2020; Maciejewska-Rutkowska et al., 2021).

5.3. Palaeobiogeographic and palaeoclimatic implications and evolution

The occurrence of *Podocarpidites*, *Phyllocladidites*, and Pinaceae during the EECO points to the existence of a diverse conifer forest in the periphery of the Xining Basin. The presence of pollen of Podocarpaceae in this region is well outside of the current range of extant *Phyllocladus* and *Podocarpus*. As bisaccate pollen can be transported over longer distances due to the buoyancy effect (Leslie, 2010; Schwendemann et al., 2007), the presence of pollen alone is not conclusive proof for the presence of the parent plant in this exact location. However, dispersal varies between species, and evidence from pollen spectra in New Zealand suggests that *Phyllocladus* pollen does not disperse very far from the parent plants (Pocknall, 1982). Given the strong similarities between fossil and modern pollen morphology, we assume that the *Phyllocladidites* specimens originated from plants in close proximity. Our findings thus extend the presence of both pollen genera in Central Asia from the Cretaceous (Zhang and Zhan, 1991; Wang et al., 1990) to the Eocene.

Phyllocladus and *Parcisporites* are of presumed Gondwanan origin, and possibly first reached Central Asia — including NE Tibet — during the successive accretions of the Qiangtang Terrane and of the Lhasa Terrane during the early Jurassic and earliest Cretaceous respectively (Kapp & Decelles, 2019; Tian et al., 2022). According to Morley (2011) and Wagstaff (2004), the Podocarpaceae were more diverse and widespread during the Jurassic,

including the Northern hemisphere, but were mainly distributed in Gondwana from the Early Cretaceous to the present day. Morley (2011) also placed the wider distribution and diversity of Podocarpaceae before the speciation of modern *Phyllocladus*, which would have appeared during the Palaeogene in Australia and Patagonia, dispersing northwards to Borneo by the Pleistocene. Based on genetic evidence, Wagstaff (2004) suggested that whilst the genus was more diverse and widespread during the Palaeogene, the ancestor of the five extant species of *Phyllocladus* would have radiated only recently during the Neogene (ca. 6.3 Ma). However, a recent molecular study of the Podocarpaceae by Chen et al. (2022) places the origination of the Prumnopityoid group of podocarps (including *Phyllocladus*), and the subsequent speciation of *Phyllocladus* and its nearest relative *Lepidothamnus* in the Late Jurassic (over 150 Ma). Therefore, it is likely that the *Phyllocladidites* in the Xining Basin corresponds to a close relative of modern *Phyllocladus*. Widespread extinctions of *Phyllocladus* and *Podocarpus* species throughout the Cenozoic could explain the disparity between past and modern ranges and diversity (Crisp & Cook, 2011; Wagstaff, 2004).

The start of the EECO was marked by a decrease of gymnosperms in favour of increasing angiosperm pollen, a pattern that was observed both in our Tibetan section and in New Zealand, where *Podocarpidites,* and gymnosperms in general, were highly abundant prior to the EECO (Crouch et al., 2020; Pocknall, 1990). For New Zealand, Crouch et al. (2020) reported a slight increase in *Podocarpidites* during the EECO, which then decreased to its lowest point by the end of the EECO but continued to linger on thereafter. This contrasts with our findings from Tibet where *Podocarpidites* nearly disappeared after the EECO, indicating the genus is less suited to post-EECO climatic conditions in Tibet as opposed to those in New Zealand. Similarly, in Patagonia, *Phyllocladidites* reportedly became extinct after the Miocene Climatic Optimum (MCO), possibly due to increasingly cool and arid conditions,

whilst *Podocarpidites* remained, although it was very reduced in range (Barreda & Palazzesi, 2007). Additional evidence from Patagonia suggests that an ancient relative of *Phyllocladus*, *Huncocladus*, was present prior to the Eocene, and subsequently went extinct during the post-Eocene trend of cooling and aridification due to the genus's low tolerance for aridity (Andruchow-Colombo et al., 2019). *Podocarpidites* populations are also reported to have increased in Antarctica during the MCO, indicating that temperatures at the poles were at the time still sufficiently high, possibly with a low of roughly 10°C during winter (Warny et al., 2009), which falls within the range of lowest temperatures of *Podocarpus* (cf. Fig. 8). Evidence from East Asia points towards rapid climatic change in the later part of the early Eocene, including a decline in temperature and precipitation (Zhang et al., 2022). Additionally, a reason the New Zealand podocarp forests may have fared better than Tibetan populations is that the former experienced relatively milder climatic conditions due to the ocean acting as a buffer (Coomes & Bellingham, 2011). This would have likely impacted podocarp distributions, as modern podocarps are known to not tolerate extreme cold or drought conditions (Coomes & Bellingham, 2011).

The presence of the *Phyllocladidites* and *Podocarpidites* in the periphery of the Xining Basin leads us to suspect that temperatures warmer than present and precipitation higher than present favoured podocarp forest presence during the EECO. Given the co-occurrence of *Phyllocladus* and *Podocarpus* and their similar climatic preferences, fossil *Podocarpidites* likely occurred throughout and beyond the range of *Phyllocladidites*, and would have had a much broader distribution. The increasingly cool and arid conditions throughout the Cenozoic may have resulted in the retreat of their distribution ranges and reduction of their diversification rate.

6. Conclusion

Our palynological study of sediments of early Eocene age from the NE Tibetan Plateau confirms the presence of *Phyllocladidites* and *Podocarpidites* pollen, and we note the strong similarity of the former with *Parcisporites*. The botanical affinity of *Phyllocladidites is Phyllocladus*, a conifer that is nowadays restricted to southern hemisphere, warm-temperate forests. Based on the presence of this taxon, together with other Podocarpaceae, we conclude that climate conditions in this area were relatively warmer and more humid than present, which is in line with what is known of climatic conditions during the EECO in Tibet. This implies that Podocarpaceae distribution was much broader during the EECO than it is today. Such wide differences in geographic distribution may be explained through possible widespread extinction of these podocarps as a result of cooling after the EECO, especially in the case of taxa related to the extant genus *Phyllocladus*. Our data supports that climatic optima stand out as periods linked to important vegetational changes and are likely connected to the range expansions and extirpation of tropical and sub-tropical species, including our southern gymnosperms, at the end of the EECO when cooling was initiated. Our findings on *Phyllocladidites* contribute to our understanding of their biogeographical history and invite further work to untangle the story of tropical gymnosperms through time.

Data Availability

Confocal and Airyscan Images of this project are available from Open Science Framework (osf.io) under DOI 10.17605/OSF.IO/CMNEJ.

Acknowledgements

We are grateful to the Botanical Garden in Bonn and its gardeners facilitating access to the living collection of podocarps for photographic documentation, and Naturalis Biodiversity

Center for providing microscopic slides on loan. We further thank Helma Kuijpers and Kèvin Knoops of the Microscopy CORE lab (University of Maastricht) for their support with confocal microscopy. We are very grateful to Christiane Wenske and Ulrich Heimhofer (Leibniz University Hannover) who provided access to lab and microscope equipment. We also thank Rudolf Bauerfeind (Medizinische Hochschule Hannover) and Ingrid Romero for their insightful support with Airyscan microscopy. and Yaron Malkowsky (University of Bonn) for his support with scanning electron microscopy (SEM). JG acknowledges funding for SEM from the DFG, project nr. 471591895. Finally, we thank the anonymous reviewer for their valuable feedback.

References

Altmann, T., Damm, B., Frommer, W., Martin, T., Morris, P., Schweizer, D., Willmitzer, L., Schmidt, R., 1994. Easy determination of ploidy level in *Arabidopsis thaliana* plants by means of pollen size measurement. Plant Cell Reports 13 (11), 652–656. https://doi.org/10.1007/BF00232939

Andruchow-Colombo, A., Wilf, P., Escapa, I. H., 2019. A South American fossil relative of *Phyllocladus*: *Huncocladus laubenfelsii* gen. et sp. nov. (Podocarpaceae), from the early Eocene of Laguna del Hunco, Patagonia, Argentina. Australian Systematic Botany 32 (4), 290–309. https://doi.org/10.1071/SB18043

Barbolini, N., Woutersen, A., Dupont-Nivet, G., Silvestro, D., Tardif, D., Coster, P. M. C., Meijer, N., Chang, C., Zhang, H. X., Licht, A., Ryan, C., Koutsodendris, A., Han, F., Rohrmann, A., Liu, X. J., Zhang, Y., Dormaaied, Y., Fluteau, F., Ladant, J. B., Le Hir, G., Hoorn, C., 2020. Cenozoic evolution of the steppe-desert biome in Central Asia. Science Advances 6 (41). https://doi.org/10.1126/SCIADV.ABB8227

Barreda, V., Palazzesi, L., 2007. Patagonian vegetation turnovers during the Paleogene-Early Neogene: Origin of arid-adapted floras. The Botanical Review 73 (1), 31–50. https://doi.org/10.1663/0006-8101(2007)73[31:PVTDTP]2.0.CO;2

Berry, K., 2022. A *Classopollis* "spike" in the *Rugubivesiculites* Zone of the Kayan Sandstone, western Sarawak, Borneo, suggests a Danian age for these deposits. Review of Palaeobotany and Palynology 304, 104728. https://doi.org/10.1016/j.revpalbo.2022.104728

Biffin, E., Brodribb, T. J., Hill, R. S., Thomas, P., Lowe, A. J., 2012. Leaf evolution in Southern Hemisphere conifers tracks the angiosperm ecological radiation. Proceedings of the Royal Society B: Biological Sciences 279 (1727), 341–348. https://doi.org/10.1098/RSPB.2011.0559

Bogotá-Ángel, G., Huang, H., Jardine, P. E., Chazot, N., Salamanca, S., Banks, H., Pardo-Trujillo, A., Plata, A., Dueñas, H., Star, W., Langelaan, R., Eisawi, A., Umeji, O. P., Enuenwemba, L. O., Parmar, S., Da Silveira, R. R., Lim, J. Y., Prasad, V., Morley, R. J., Bacon, C. D., Hoorn, C., 2021. Climate and geological change as drivers of Mauritiinae palm biogeography. Journal of Biogeography 48, 1001–1022. https://doi.org/10.1111/jbi.14098

Bosboom, R. E., Abels, H. A., Hoorn, C., van den Berg, B. C. J., Guo, Z. J., Dupont-Nivet, G., 2014. Aridification in continental Asia after the Middle Eocene Climatic Optimum (MECO). Earth and Planetary Science Letters 389, 34–42. https://doi.org/10.1016/J.EPSL.2013.12.014

Botsyun, S., Sepulchre, P., Donnadieu, Y., Risi, C., Licht, A., Caves Rugenstein, J. K., 2019. Revised paleoaltimetry data show low Tibetan Plateau elevation during the Eocene. Science 363 (6430). https://doi.org/10.1126/SCIENCE.AAQ1436

Burke, K. D., Williams, J. W., Chandler, M. A., Haywood, A. M., Lunt, D. J., Otto-Bliesner, B. L., 2018. Pliocene and Eocene provide best analogs for near-future climates. Proceedings of the National Academy of Sciences of the United States of America 115 (52), 13288–13293. https://doi.org/10.1073/PNAS.1809600115

Chen, J., Du, S., Chen, C., Liu, F., Ning, Z., Song, X., Liu, S., Lu, H., Liu, Y., Kuang, H., 2019. A research of the Cretaceous-Paleogene Boundary in the Pingyi Basin, Shandong Province. Open Journal of Geology 09 (10), 661–664. https://doi.org/10.4236/ojg.2019.910068

Chen, L., Jin, W.-T., Liu, X.-Q., Wang, X.-Q., 2022. New insights into the phylogeny and evolution of Podocarpaceae inferred from transcriptomic data. Molecular Phylogenetics and Evolution 166, 107341. https://doi.org/10.1016/j.ympev.2021.107341

Clark, M. K., Farley, K. A., Zheng, D., Wang, Z., Duvall, A. R., 2010. Early Cenozoic

faulting of the northern Tibetan Plateau margin from apatite (U–Th)/He ages. Earth and Planetary Science Letters 296 (1-2), 78-88. https://doi.org/10.1016/j.epsl.2010.04.051

Cookson, I. C., 1947. Plant microfossils from the lignites of Kerguelen Archipelago. B.A.N.Z. Antarctica Research Expedition Report 2 (8), 130–142.

Coomes, D. A., Bellingham, P. J., 2011. Temperate and Tropical Podocarps: How Ecologically Alike Are They? In Turner, B. L., Cernusak, L. A. (Eds.), Ecology of the Podocarpaceae in Tropical Forests, 119–140. Smithsonian Institution Scholarly Press. https://doi.org/10.5479/SI.0081024X.95.119

Couper, R. A., 1953. Upper Mesozoic and Cainozoic spores and pollen grains from New Zealand. New Zealand Geological Survey Paleontological Bulletin 22, 1–77.

Coxall, H. K., Wilson, P. A., Pälike, H., Lear, C. H., Backman, J., 2005. Rapid stepwise onset of Antarctic glaciation and deeper calcite compensation in the Pacific Ocean. Nature 433 (7021), 53–57. https://doi.org/10.1038/NATURE03135

Cramwinckel, M. J., Huber, M., Kocken, I. J., Agnini, C., Bijl, P. K., Bohaty, S. M., Frieling, J., Goldner, A., Hilgen, F. J., Kip, E. L., Peterse, F., Van Der Ploeg, R., Röhl, U., Schouten, S., Sluijs, A., 2018. Synchronous tropical and polar temperature evolution in the Eocene. Nature 559, 382–386 https://doi.org/10.1038/s41586-018-0272-2

Crisp, M. D., Cook, L. G., 2011. Cenozoic extinctions account for the low diversity of extant gymnosperms compared with angiosperms. New Phytologist 192 (4), 997–1009. https://doi.org/10.1111/J.1469-8137.2011.03862.X

Crouch, E. M., Shepherd, C. L., Morgans, H. E. G., Naafs, B. D. A., Dallanave, E., Phillips, A., Hollis, C. J., Pancost, R. D., 2020. Climatic and environmental changes across the early Eocene climatic optimum at mid-Waipara River, Canterbury Basin, New Zealand. Earth-Science Reviews 200, 102961. https://doi.org/10.1016/J.EARSCIREV.2019.102961

Cui, Y., Gong, E. P., Wang, T. H., Guan, C. Q., Zhang, Y. L., Liang, J. H., 2015. Palynomorph assemblages and paleoclimate records from the Zhuanchengzi Bed of the Yixian Formation, western Liaoning Province, China. Science China Earth Sciences 58 (9), 1538–1552. https://doi.org/10.1007/S11430-015-5147-X

De Storme, N., Zamariola, L., Mau, M., Sharbel, T. F., Geelen, D., 2013. Volume-based pollen size analysis: An advanced method to assess somatic and gametophytic ploidy in flowering plants. Plant Reproduction 26 (2), 65–81. https://doi.org/10.1007/s00497-012-0209-0

de Wet, J. M. J., 1971. Polyploidy and evolution in plants. Taxon 20 (1), 29–35.

Dupont-Nivet, G., Hoorn, C., Konert, M., 2008. Tibetan uplift prior to the Eocene-Oligocene climate transition: Evidence from pollen analysis of the Xining Basin. Geology 36 (12), 987–990. https://doi.org/10.1130/G25063A.1

Erdtman, G., 1957. Pollen and spore morphology/plant taxonomy; gymnospermae, pteriodophyta, bryophyta (Illustrations). Almqvist & Wiksell. https://doi.org/10.5962/bhl.title.5693

Ejsmond, M. J., Wrońska-Pilarek, D., Ejsmond, A., Dragosz-Kluska, D., Karpińska-Kołaczek, M., Kołaczek, P., Kozłowski, J., 2011. Does climate affect pollen morphology? Optimal size and shape of pollen grains under various desiccation intensity. Ecosphere 2 (10), 117. https://doi.org/10.1890/ES11-00147.1

Escudero, M., Martín-Bravo, S., Mayrose, I., Fernández-Mazuecos, M., Fiz-Palacios, O., Hipp, A. L., Pimentel, M., Jiménez-Mejías, P., Valcárcel, V., Vargas, P., Luceño, M., 2014. Karyotypic changes through dysploidy persist longer over evolutionary time than polyploid changes. PLoS ONE, 9 (1). https://doi.org/10.1371/journal.pone.0085266

Fatmi, H., Maalem, S., Harsa, B., Dekak, A., Chenchouni, H., 2020. Pollen morphological variability correlates with a large-scale gradient of aridity. Web Ecology 20 (1), 19–32.

https://doi.org/10.5194/we-20-19-2020

Falcon-Lang, H. J., Fensome, R. A., Venugopal, D. V., 2003. The Cretaceous age of the Vinegar Hill silica sand deposit, southern New Brunswick: Evidence from palynology and paleobotany. Atlantic Geology 39 (1), 39–46. https://doi.org/10.4138/1048

Fensome, R. A., Williams, G. L., MacRae, R. A., 2019. The Lentin and Williams index of fossil dinoflagellates: 2019 edition. American Association of Stratigraphic Palynologists Contributions Series 50, 1173pp.

GBIF.org., 2022a. GBIF Occurence Download. https://doi.org/10.15468/dl.2a2nyz

GBIF.org., 2022b. GBIF Occurence Download. https://doi.org/10.15468/dl.es8dx4

Gernandt, D. S., Magallón, S., Geada López, G., Zerón Flores, O., Willyard, A., Liston, A., 2008. Use of Simultaneous Analyses to Guide Fossil-Based Calibrations of Pinaceae Phylogeny. International Journal of Plant Sciences 169 (8), 1086–1099. https://doi.org/10.1086/590472

Goodhue, R., Clayton, G., 2010. Palynomorph darkness index (PDI) - A new technique for assessing thermal maturity. Palynology 34 (2), 147–156. https://doi.org/10.1080/01916121003696932

Gradstein, F. M., Ogg, J. G., 2020. Geologic time scale 2020 (1st ed.). Elsevier.

Gravendyck, J., 2021. Shedding new Light on the Triassic-Jurassic Transition in the Germanic Basin: Novel insights from the Bonenburg section & palynotaxonomy and nomenclature of plant microfossils [Freie Universität Berlin]. In ReFUbium. https://doi.org/http://dx.doi.org/10.17169/refubium-31383.

Gravendyck, J., Fensome, R. A., Coiffard, C., Bachelier, J. B., 2022a. Assessing taxon names in palynology (I): Working with databases. Palynology 46 (3), 1–11. https://doi.org/10.1080/01916122.2022.2026834

Gravendyck, J., Coiffard, C., Bachelier, J. B., 2022b. Assessing taxon names in palynology

(II): Indices to quantify use of names. Palynology 46 (3), in print. https://doi.org/10.1080/01916122.2022.2034675

Gravendyck, J., Coiffard, C., Bachelier, J. B., Kürschner, W., in press. Re-evaluation of *Cerebropollenites thiergartii* Eberh. Schulz 1967 and related taxa: priority of *Sciadopityspollenites* and nomenclatural novelties. Grana. https://doi.org/10.1080/00173134.2022.2158688

Greenwood, D. R., Wing, S. L., 1995. Eocene continental climates and latitudinal temperature gradients. Geology 23 (11), 1044–1048. https://doi.org/10.1130/0091-7613(1995)023<1044:ECCALT>2.3.CO;2

Han, F., Rydin, C., Bolinder, K., Dupont-Nivet, G., Abels, H. A., Koutsodendris, A., Zhang, K., Hoorn, C., 2016. Steppe development on the Northern Tibetan Plateau inferred from Paleogene ephedroid pollen. Grana 55 (1), 73–100. https://doi.org/10.1080/00173134.2015.1120343

Haslett, J., Parnell, A., 2008. A simple monotone process with application to radiocarbon-dated depth chronologies. Journal of the Royal Statistical Society: Series C (Applied Statistics) 57 (4), 399–418. https://doi.org/10.1111/j.1467-9876.2008.00623.x

Hoorn, C., Straathof, J., Abels, H. A., Xu, Y., Utescher, T., Dupont-Nivet, G., 2012. A late Eocene palynological record of climate change and Tibetan Plateau uplift (Xining Basin, China). Palaeogeography, Palaeoclimatology, Palaeoecology 344–345, 16–38. https://doi.org/10.1016/J.PALAEO.2012.05.011

Horton, B. K., Dupont-Nivet, G., Zhou, J., Waanders, G. L., Butler, R. F., Wang, J., 2004. Mesozoic-Cenozoic evolution of the Xining-Minhe and Dangchang basins, northeastern Tibetan Plateau: Magnetostratigraphic and biostratigraphic results. Journal of Geophysical Research 109, 4402. https://doi.org/10.1029/2003JB002913

Huang, H., Morley, R., Licht, A., Dupont-Nivet, G., Grímsson, F., Zetter, R., Westerweel, J.,

Zaw, W. I. N., Aung, D. W. A., Hoorn, C., 2020. Eocene palms from central Myanmar in a South-East Asian and global perspective: evidence from the palynological record. Botanical Journal of the Linnean Society 194 (2), 177–206. https://doi.org/10.1093/BOTLINNEAN/BOAA038

Huber, B. T., MacLeod, K. G., Watkins, D. K., Coffin, M. F., 2018. The rise and fall of the Cretaceous Hot Greenhouse climate. Global and Planetary Change 167, 1–23. https://doi.org/10.1016/J.GLOPLACHA.2018.04.004

Huff, J., 2015. The Airyscan detector from ZEISS: Confocal imaging with improved signal-to-noise ratio and super-resolution. Nature Methods 12 (12), ii. https://doi.org/10.1038/NMETH.F.388

Huff, J., Bergter, A., Luebbers, B., 2019. Application Note: Multiplex mode for the LSM 9 series with Airyscan 2: Fast and gentle confocal super-resolution in large volumes. Nature Methods (October).

Inglis, G. N., Bragg, F., Burls, N. J., Cramwinckel, M. J., Evans, D., Foster, G. L., Huber, M., Lunt, D. J., Siler, N., Steinig, S., Tierney, J. E., Wilkinson, R., Anagnostou, E., M. De Boer, A., Dunkley Jones, T., Edgar, K. M., Hollis, C. J., Hutchinson, D. K., Pancost, R. D., 2020. Global mean surface temperature and climate sensitivity of the early Eocene Climatic Optimum (EECO), Paleocene-Eocene Thermal Maximum (PETM), and latest Paleocene. Climate of the Past 16 (5), 1953–1968. https://doi.org/10.5194/CP-16-1953-2020

Jansonius, J., Hills, L. V., 1976. Genera File of Fossil Spores and Pollen Special Publication. Department of Geology, University of Calgary.

Kapp, P., Decelles, P. G., 2019. Mesozoic–Cenozoic geological evolution of the Himalayan-Tibetan orogen and working tectonic hypotheses. American Journal of Science 319 (3), 159–254. https://doi.org/10.2475/03.2019.01

Kaya, M. Y., Dupont-Nivet, G., Proust, J. N., Roperch, P., Bougeois, L., Meijer, N., Frieling, J., Fioroni, C., Özkan Altıner, S., Vardar, E., Barbolini, N., Stoica, M., Aminov, J., Mamtimin, M., Zhaojie, G., 2019. Paleogene evolution and demise of the proto-Paratethys Sea in Central Asia (Tarim and Tajik basins): Role of intensified tectonic activity at ca. 41 Ma. Basin Research 31 (3), 461–486. https://doi.org/10.1111/BRE.12330

Kelly, A. E., Goulden, M. L., 2008. Rapid shifts in plant distribution with recent climate change. Proceedings of the National Academy of Sciences of the United States of America 105 (33), 11823–11826. https://doi.org/10.1073/PNAS.0802891105

Keng, H., 1973. On the family Phyllocladaceae. Taiwania 18 (2), 142–145. https://doi.org/10.6165/tai.1973.18.142

Keng, H., 1978. The genus *Phyllocladus* (Phyllocladaceae). Journal of the Arnold Arboretum 59 (3), 249–273. https://www.jstor.org/stable/43782044

Khoshoo, T. N., 1961. Chromosome numbers in gymnosperms. Silvae Genetica 10 (1), 1–9.

Korasidis, V. A., Wallace, M. W., Wagstaff, B. E., Hill, R. S., 2019. Terrestrial cooling record through the Eocene–Oligocene transition of Australia. Global and Planetary Change 173, 61–72. https://doi.org/10.1016/J.GLOPLACHA.2018.12.007

Leschik, G., 1955. Die Keuperflora von Neuewelt bei Basel. II. Die Iso- und Mikrosporen. Schweizerische Paläontologische Abhandlungen 72, 1–70.

Leslie, A. B., 2010. Flotation preferentially selects saccate pollen during conifer pollination. New Phytologist 188 (1), 273–279. https://doi.org/10.1111/J.1469-8137.2010.03356.X

Leslie, A. B., Beaulieu, J. M., Rai, H. S., Crane, P. R., Donoghue, M. J., Mathews, S., 2012. Hemisphere-scale differences in conifer evolutionary dynamics. Proceedings of the National Academy of Sciences 109(40), 16217–16221. https://doi.org/10.1073/pnas.1213621109

Li, J., Wu, Y., Peng, J., Batten, D. J., 2019. Palynofloral evolution on the northern margin of the Indian Plate, southern Xizang, China during the Cretaceous Period and its phytogeographic significance. Palaeogeography, Palaeoclimatology, Palaeoecology 515, 107–122. https://doi.org/10.1016/J.PALAEO.2017.09.014

Li, Y., Sun, P., Falcon-Lang, H. J., Liu, Z., Zhang, B., Zhang, Q., Wang, J., Xu, Y., 2022. Eocene Hyperthermal events drove episodes of vegetation turnover in the Fushun Basin, Northeast China: Evidence from a palaeoclimate analysis of palynological assemblages. SSRN Electronic Journal. https://doi.org/10.2139/SSRN.4192876

Lim, J. Y., Huang, H., Farnsworth, A., Lunt, D. J., Baker, W. J., Morley, R. J., Kissling, W. D., Hoorn, C., 2022. The Cenozoic history of palms: Global diversification, biogeography and the decline of megathermal forests. Global Ecology and Biogeography 31, 425–439. https://doi.org/10.1111/geb.13436

Ma, X., Jiang, H., Cheng, J., Xu, H., 2012. Spatiotemporal evolution of Paleogene palynoflora in China and its implication for development of the extensional basins in East China. *Review of* Palaeobotany and Palynology 184, 24–35. https://doi.org/10.1016/J.REVPALBO.2012.07.013

Maciejewska-Rutkowska, I., Bocianowski, J., Wrońska-Pilarek, D., 2021. Pollen morphology and variability of Polish native species from genus Salix L. PLoS ONE 16 (2 February), 1–22. https://doi.org/10.1371/journal.pone.0243993

Meijer, N., Dupont-Nivet, G., Licht, A., Roperch, P., Rohrmann, A., Sun, A., Lu, S., Woutersen, A., Nowaczyk, N., 2022. Early Eocene magnetostratigraphy and tectonic evolution of the Xining Basin, NE Tibet. Basin Research 00, 1-20. https://doi.org/https://doi.org/10.1111/bre.12720

Mildenhall, D. C., 1980. New Zealand late Cretaceous and Cenozoic plant biogeography: A contribution. Palaeogeography, Palaeoclimatology, Palaeoecology 31(C), 197–233.

https://doi.org/10.1016/0031-0182(80)90019-X

Miller, K. G., Wright, J. D., Fairbanks, R. G., 1991. Unlocking the Ice House: Oligocene-Miocene oxygen isotopes, eustasy, and margin erosion. Journal of Geophysical Research: Solid Earth 96(B4), 6829–6848. https://doi.org/10.1029/90JB02015

Molloy, B. P. J., Markham, K. R., 1999. A contribution to the taxonomy of *Phyllocladus* (Phyllocladaceae) from the distribution of key flavonoids. New Zealand Journal of Botany 37 (3), 375–382. https://doi.org/10.1080/0028825X.1999.9512642

Moran, E. V., Thuiller, W., Angert, A. L., Benito Garzón, M., 2022. Editorial: Predicting and managing climate-driven range shifts in plants. Frontiers in Ecology and Evolution 10, 153. https://doi.org/10.3389/FEVO.2022.856213

Morley, R. J., 2011. Dispersal and paleoecology of tropical Podocarps. In Turner, B. L., Cernusak, L. A. (Eds.), Ecology of the Podocarpaceae in Tropical Forests, 21–41. Smithsonian Institution Scholarly Press. https://doi.org/10.5479/SI.0081024X.95.21

Page, C. N., 1990. Phyllocladaceae. In Kramer, K. U., Green, P. S. (Eds.), The Families and Genera of Vascular Plants, 317–319. Springer, Berlin, Heidelberg. https://doi.org/10.1007/978-3-662-02604-5_57

Page, M., Licht, A., Dupont-Nivet, G., Meijer, N., Barbolini, N., Hoorn, C., Schauer, A., Huntington, K., Bajnai, D., Fiebig, J., Mulch, A., Guo, Z., 2019. Synchronous cooling and decline in monsoonal rainfall in northeastern Tibet during the fall into the Oligocene icehouse. Geology 47 (3), 203–206. https://doi.org/10.1130/G45480.1

Palynodata Inc., White, J. M., 2008. Palynodata Datafile: 2006 version. In Natural Resources Canada (p. Open File 5793, 1 CD-ROM). https://doi.org/10.4095/225704

Pieńkowski, G., Niedźwiedzki, G., Waksmundzka, M., 2012. Sedimentological, palynological and geochemical studies of the terrestrial Triassic-Jurassic boundary in northwestern Poland. Geological Magazine 149 (2), 308–332.

https://doi.org/10.1017/S0016756811000914

Pocknall, D. T., 1981. Pollen morphology of *Phyllocladus* L. C. et A. Rich. New Zealand Journal of Botany 19, 259–266. https://doi.org/10.1080/0028825X.1981.10426378

Pocknall, D. T., 1982. Modern pollen spectra from mountain localities, South Island, New Zealand. NZ Journal of Botany 20, 361-371. https://doi.org/10.1080/0028825X.1982.10428505

Pocknall, D. T., 1990. Palynological evidence for the early to middle Eocene vegetation and climate history of New Zealand. Review of Palaeobotany and Palynology 65 (1–4), 57–69. https://doi.org/10.1016/0034-6667(90)90056-O

Praglowski, J., 1970. The effects of pre-treatment and the embedding media on the shape of pollen grains. Review of Palaeobotany and Palynology 10 (3), 203–208. https://doi.org/10.1016/0034-6667(70)90065-5

R Core Team., 2021. R: A language and environment for statistical computing. R Foundation for Statistical Computing. https://www.r-project.org/

Romero, I. C., Kong, S., Fowlkes, C. C., Jaramillo, C., Urban, M. A., Oboh-Ikuenobe, F., D'apolito, C., Punyasena, S. W., 2020a. Improving the taxonomy of fossil pollen using convolutional neural networks and superresolution microscopy. PNAS 117 (45), 28496–28505. https://doi.org/10.1073/pnas.2007324117

Romero, I. C., Urban, M. A., Punyasena, S. W., 2020b. Airyscan superresolution microscopy: A high-throughput alternative to electron microscopy for the visualization and analysis of fossil pollen. Review of Palaeobotany and Palynology, 276. https://doi.org/10.1016/j.revpalbo.2020.104192

RStudio Team., 2021. RStudio: Integrated Development Environment for R. RStudio, PBC. http://www.rstudio.com/

Rueden, C. T., Schindelin, J., Hiner, M. C., DeZonia, B. E., Walter, A. E., Arena, E. T., &

Eliceiri, K. W, 2017. ImageJ2: ImageJ for the next generation of scientific image data. BMC Bioinformatics 18 (1), 529. https://doi.org/10.1186/s12859-017-1934-z

Schindelin, J., Arganda-Carreras, I., Frise, E., Kaynig, V., Longair, M., Pietzsch, T., Preibisch, S., Rueden, C., Saalfeld, S., Schmid, B., Tinevez, J.-Y., White, D. J., Hartenstein, V., Eliceiri, K., Tomancak, P., Cardona, A., 2012. Fiji: an open-source platform for biological-image analysis. Nature Methods 9 (7), 676–682. https://doi.org/10.1038/nmeth.2019

Schrank, E., 2010. Pollen and spores from the Tendaguru Beds, Upper Jurassic and Lower Cretaceous of southeast Tanzania: Palynostratigraphical and paleoecological implications. Palynology 34 (1), 3–42. https://doi.org/10.1080/01916121003620106

Schwendemann, A. B., Wang, G., Mertz, M. L., McWilliams, R. T., Thatcher, S. L., Osborn, J. M., 2007. Aerodynamics of saccate pollen and its implications for wind pollination. American Journal of Botany 94 (8), 1371–1381. https://doi.org/10.3732/ajb.94.8.1371

Sivaguru, M., Urban, M. A., Fried, G., Wesseln, C. J., Mander, L., Punyasena, S. W., 2018. Comparative performance of airyscan and structured illumination superresolution microscopy in the study of the surface texture and 3D shape of pollen. Microscopy Research and Technique 81 (2), 101–114. https://doi.org/10.1002/jemt.22732

Sluyter, A., 1997. Analysis of maize (*Zea mays* subsp *mays*) pollen: Normalizing the effects of microscope-slide mounting media on diameter determinations. Palynology 21 (1), 35–39. https://doi.org/10.1080/01916122.1997.9989485

Song, Z., Zheng, Y., Li, J., Ye, P., Wang, C. F., Zhou, S. F., 1985. Cretaceous-Tertiary Palynological Assemblages from Jiangsu. Geological Publishing House.

Song, Z., Zheng, Y., Li, M., Zhang, Y., Wang, W.-M., Wang, D., Zhao, C., Shanfu, Z., Zhu, Z., Zhao, Y., 1999. Fossil Spores and Pollen of China (Volume 1): The Late Cretaceous and Tertiary Spores and Pollen. Science Press, Beijing.

Spicer, R. A., Su, T., Valdes, P. J., Farnsworth, A., Wu, F. X., Shi, G., Spicer, T. E. V., Zhou, Z., 2021. Why 'the uplift of the Tibetan Plateau' is a myth. National Science Review 8 (1), 2021. https://doi.org/10.1093/NSR/NWAA091

Srisuwan, S., Sihachakr, D., Martín, J., Vallès, J., Ressayre, A., Brown, S. C., Siljak-Yakovlev, S., 2019. Change in nuclear DNA content and pollen size with polyploidisation in the sweet potato (*Ipomoea batatas*, Convolvulaceae) complex. Plant Biology 21 (2), 237–247. https://doi.org/10.1111/plb.12945

Staplin, F. L., 1969. Sedimentary organic matter, organic metamorphism, and oil and gas occurrence. Bulletin of Canadian Petroleum Geology 17 (1), 47–66.

Su, T., Spicer, R. A., Li, S. H., Xu, H., Huang, J., Sherlock, S., Huang, Y. J., Li, S. F., Wang, L., Jia, L. B., Deng, W. Y. D., Liu, J., Deng, C. L., Zhang, S. T., Valdes, P. J., Zhou, Z. K., 2019. Uplift, climate and biotic changes at the Eocene-Oligocene transition in south-eastern Tibet. National Science Review 6 (3), 495–504. https://doi.org/10.1093/NSR/NWY062

Su, L., Zhang, Q., Sun, Y., Zhang, S., Smith, T., Li, C., 2022. New evidence of the emergence of East Asian monsoon in the early Palaeogene. Scientific Reports 12 (20471). https://doi.org/10.1038/s41598-022-24298-z

Tapponnier, P., Zhiqin, X., Roger, F., Meyer, B., Arnaud, N., Wittlinger, G., & Jingsui, Y. (2001). Oblique stepwise rise and growth of the Tibet Plateau. Science 294 (5547), 1671–1677. https://doi.org/10.1126/SCIENCE.105978

Tian, Z., Zhang, Z., Piccoli, P. M., Dong, X., 2022. Early Jurassic accretion of retrograde eclogites and granulites in the Amdo complex, Bangong–Nujiang suture zone, central Tibet. Gondwana Research 104, 70–91. https://doi.org/10.1016/J.GR.2021.08.010

Tomlinson, P. B., Braggins, J. E., Rattenbury, J. A., 1997. Contrasted pollen capture mechanisms in Phyllocladaceae and certain Podocarpaceae (Coniferales). American

Journal of Botany 84 (2), 214–223. https://doi.org/10.2307/2446083

Traverse, A., 2007. Spores/Pollen Morphology. In Paleopalynology: Topics in Geobiology, 87–154. Springer, Dordrecht. https://doi.org/10.1007/978-1-4020-5610-9_5

Trayler, R. B., Schmitz, M. D., Cuitiño, J. I., Kohn, M. J., Bargo, M. S., Kay, R. F., Strömberg, C. A. E., Vizcaíno, S. F., 2019. An improved approach to age-modeling in deep time: Implications for the Santa Cruz Formation, Argentina. Geological Society of America Bulletin 132, 233–244. https://doi.org/10.1130/B35203.1

van de Schootbrugge, B., Quan, T. M., Lindström, S., Püttmann, W., Heunisch, C., Pross, J., Fiebig, J., Petschick, R., Röhling, H. G., Richoz, S., Rosenthal, Y., Falkowski, P. G., 2009. Floral changes across the Triassic/Jurassic boundary linked to flood basalt volcanism. Nature Geoscience 2 (8), 589–594. https://doi.org/10.1038/ngeo577

Wagstaff, S. J., 2004. Evolution and biogeography of the austral genus *Phyllocladus* (Podocarpaceae). Journal of Biogeography 31 (10), 1569–1577. https://doi.org/10.1111/J.1365-2699.2004.01066.X

Walker, J. D., Geissman, J. W., Bowring, S. A., Babcock, L. E., 2018. Geologic Time Scale v. 5.0. Geological Society of America. https://doi.org/10.1130/2018.CTS005R3C

Wang, C., Dai, J., Zhao, X., Li, Y., Graham, S. A., He, D., Ran, B., Meng, J., 2014a. Outward-growth of the Tibetan Plateau during the Cenozoic: A review. Tectonophysics 621, 1–43. https://doi.org/10.1016/J.TECTO.2014.01.036

Wang, C., Zhao, X., Liu, Z., Lippert, P. C., Graham, S. A., Coe, R. S., Yi, H., Zhu, L., Liu, S., Li, Y., 2008. Constraints on the early uplift history of the Tibetan Plateau. Proceedings of the National Academy of Sciences of the United States of America 105 (13), 4987–4992. https://doi.org/10.1073/PNAS.0703595105

Wang, D. N., Sun, X. Y., Zhao, Y. N., He, Z., 1990. The Study on the Micropaleobotany from Cretaceous–Tertiary of the Oil Bearing Basins in Some Regions of Qinghai and

Xinjang (in Chinese with English abstract). China Environmental Science Press, Beijing, pp. 1–179.

Wang, J.-W., Chang, F., 1990. Genus *Parcisporites* and its stratigraphical significance (in Chinese with English translations of new species). Weiti Gushengwu Xuebao 7 (2), 187–192.

Wang, L., Wan, C., Sun, Y., 2014b. A spore-pollen assemblage from the Damoguaihe formation in the Tamutsag Basin, Mongolia and its geological implication. Acta Geologica Sinica 88 (1), 46–61. https://doi.org/10.1111/1755-6724.12182

Wang, N., Liu, L., Hou, X., Zhang, Y., Wei, H. and Cao, X., 2022. Palynological evidence reveals an arid early Holocene for the northeast Tibetan Plateau. Climate of the Past 18(10), 2381–2399.

Warny, S., Askin, R. A., Hannah, M. J., Mohr, B. A. R., Raine, J. I., Harwood, D. M., Florindo, F., 2009. Palynomorphs from a sediment core reveal a sudden remarkably warm Antarctica during the middle Miocene. Geology 37 (10), 955–958. https://doi.org/10.1130/G30139A.1

Wei, C., Jardine, P. E., Gosling, W. D., Hoorn, C., 2023. Is Poaceae pollen size a useful proxy in palaeoecological studies? New insights from a Poaceae pollen morphological study in the Amazon. Review of Palaeobotany and Palynology 308, 104790. https://doi.org/10.1016/J.REVPALBO.2022.104790

Weiner, J., 2020. pca3d: Three Dimensional PCA Plots. R package version 0.10.2.

Wen, J., Zhang, J.-Q., Nie, Z.-L., Zhong, Y., Sun, H., 2014. Evolutionary diversifications of plants on the Qinghai-Tibetan Plateau. Frontiers in Genetics 5. https://www.frontiersin.org/article/10.3389/fgene.2014.00004

Wesche, K., Ambarlı, D., Kamp, J., Török, P., Treiber, J., Dengler, J., 2016. The Palaearctic

steppe biome: a new synthesis. Biodiversity and Conservation 25 (12), 2197–2231. https://doi.org/10.1007/S10531-016-1214-7

Westerhold, T., Röhl, U., Donner, B., Zachos, J. C., 2018. Global extent of Early Eocene hyperthermal events: A new Pacific benthic foraminiferal isotope record from Shatsky Rise (ODP Site 1209). Paleoceanography and Paleoclimatology 33 (6), 626–642. https://doi.org/10.1029/2017PA003306

Westerhold, T., Marwan, N., Drury, A. J., Liebrand, D., Agnini, C., Anagnostou, E., Barnet, J. S. K., Bohaty, S. M., De Vleeschouwer, D., Florindo, F., Frederichs, T., Hodell, D. A., Holbourn, A. E., Kroon, D., Lauretano, V., Littler, K., Lourens, L. J., Lyle, M., Pälike, H., Röhl, U., Tian, J., Wilkens, R. H., Wilson, P. H., Zachos, J. C., 2020. An astronomically dated record of Earth's climate and its predictability over the last 66 million years. Science 369 (6509), 1383–1368. https://doi.org/10.1126/SCIENCE.ABA6853

Wickham, H., 2016. ggplot2: Elegant Graphics for Data Analysis. Springer-Verlag. https://ggplot2.tidyverse.org

Woutersen, A., Jardine, P. E., Bogotá-Ángel, R. G., Zhang, H.-X., Silvestro, D., Antonelli, A., Gogna, E., Erkens, R. H. J., Gosling, W. D., Dupont-Nivet, G., Hoorn, C., 2018. A novel approach to study the morphology and chemistry of pollen in a phylogenetic context, applied to the halophytic taxon *Nitraria* L. (Nitrariaceae). PeerJ 6. https://doi.org/10.7717/peerj.5055

Woutersen, A., Jardine, P. E., Silvestro, D., Bogotá-Ángel, R. G., Zhang, H.-X., Meijer, N., Bouchal, J., Barbolini, N., Dupont-Nivet, G., Koutsodendris, A., Antonelli, A., Hoorn, C., in press. The evolutionary history of the Central Asian steppe-desert taxon *Nitraria* L. (Nitrariaceae) as revealed by integration of fossil pollen morphology and molecular data. Botanical Journal of the Linnean Society.

Xie, Y., Wu, F., Fang, X., 2022. Abrupt collapse of a swamp ecosystem in northeast China during the Paleocene–Eocene Thermal Maximum. Palaeogeography, Palaeoclimatology, Palaeoecology 595, 110975. https://doi.org/10.1016/J.PALAEO.2022.110975

Yuan, D., Ge, W., Chen, Z., Li, C., Wang, Z., Zhang, H., Zhang, P., Zheng, D., Zheng, W., Craddock, W. H., Dayem, K. E., Duvall, A. R., Hough, B. G., Lease, R. O., Champagnac, J., Burbank, D. W., Clark, M. K., Farley, K. A., Garzione, C. N., Kirby, E., Molnar, P., Roe, G. H., 2013. The growth of northeastern Tibet and its relevance to large-scale continental geodynamics: A review of recent studies. Tectonics 32 (5), 1358–1370. https://doi.org/10.1002/tect.20081

Zhang, Y., Zhan, J., 1991. Late Cretaceous and Early Tertiary Spores and Pollen from the Western Tarim Basin, S. Xinjiang, China. Ke Xue Chu Ban She.

Zizka, A., Silvestro, D., Andermann, T., Azevedo, J., Duarte Ritter, C., Edler, D., Farooq, H., Herdean, A., Ariza, M., Scharn, R., Svantesson, S., Wengström, N., Zizka, V., & Antonelli, A., 2019. CoordinateCleaner: Standardized cleaning of occurrence records from biological collection databases. Methods in Ecology and Evolution 10 (5), 744–751. https://doi.org/10.1111/2041-210X.13152

Declaration of interests

☐The authors declare that they have no known competing financial interests or personal relationships that could have appeared to influence the work reported in this paper.

☒The authors declare the following financial interests/personal relationships which may be considered as potential competing interests:

Guillaume Dupont-Nivet, Niels Meyer, Amber Woutersen reports financial support was provided by European Research Council. co-author Huasheng Huang is co-editor of the special issue to which we are submitting

Sample name (code)	Locality	Stratigraphic position	Sample age (Ma); 95% highest density interval in brackets
17XJ-NB-207 (NB1)	Xiejia	207	43.35 (42.77-43.58)
17CJ-NB-127 (NB2)	Caijia	146.5	46.97 (46.43-47.55)
17XJ-NB-77 (NB3)	Xiejia	77	48.41 (47.97-48.78)
17XJ-NB-47 (NB4)	Xiejia	47	49.42 (49.11-49.69)
17CJ-NB-L1,5 (NB5)	Caijia	1.5	52.14 (51.81-54.41)
PEX 17-08 (P17)	East Xining	36.8	52.36 (52.11-52.57)
PEX 15-08 (P15)	East Xining	32.5	52.47 (52.24-52.65)
17BS-NB-11 (NB6)	Bingling Shan	11	52.89 (52.68-53.10)
PEX 12-08 (P12)	East Xining	20	53.02 (52.81-53.52)

ID	Herbarium sheet barcode	Collector	Collection number	Year	Locality	Species
4453940	L.1167606	J.P. van Niel	29271	n.d.	Unknown	*Phyllocladus hypophyllus*
4434841	L.1161674	Unknown	s.n.	n.d.	Unknown	*Phyllocladus trichomanoides*
4453946	L.1167613	J.P. van Niel	2748	1963	Unknown	*Podocarpus macrophyllus*

	total length	total width	corpus length	corpus width	saccus width	saccus height	saccus dist.
Phyllocladidites							
MAX (µm)	59.40	58.50	59.40	58.50	53.28	9.58	36.42
MIN (µm)	31.56	26.45	31.56	26.45	13.16	2.16	9.93
MEAN (µm)	41.55	45.37	41.41	45.37	26.64	5.14	22.09
SDEV (µm)	8.50	8.69	8.36	8.69	8.49	1.97	7.39
RMAX (%)	-	161.47	100.00	161.47	113.50	23.98	67.10
RMIN (%)	-	82.89	94.19	82.89	41.24	6.49	27.02
RAVG (%)	-	109.19	99.66	109.19	64.11	12.36	53.17
RSDEV (%)	-	19.66	1.27	19.66	19.11	4.93	11.77
Podocarpidites							
MAX (µm)	92.73	50.24	52.01	46.00	46.50	43.29	18.87
MIN (µm)	40.32	26.06	18.37	16.44	21.50	13.10	2.16
MEAN (µm)	57.74	35.06	30.85	27.92	33.18	25.07	9.62
SDEV (µm)	14.74	7.06	9.42	8.57	7.42	8.18	4.40
RMAX (%)	-	89.40	69.94	82.53	89.40	69.18	35.51
RMIN (%)	-	40.72	39.84	28.59	38.67	26.36	5.36
RAVG (%)	-	60.71	53.42	48.36	57.46	43.42	16.65

Northward expansion of the southern-temperate podocarp forest during the Early Eocene Climatic Optimum: Palynological evidence from the NE Tibetan Plateau (China)

Robin-Champigneul, Faez [a*]; Gravendyck, Julia [b,c]; Huang, Huasheng[d]; Woutersen, Amber [e]; Pocknall, David [f]; Meijer, Niels [g]; Dupont-Nivet, G. [h]; Erkens, Roy H. J. [a,i]; Hoorn, C. [e*]

Highlights

- We studied gymnosperm pollen of early Eocene sediments in NE Tibet
- *Phyllocladidites* (affinity *Phyllocladus*) and *Podocarpidites* were common
- Now, *Phyllocladus* is restricted to temperate forests in the southern hemisphere
- Their extent into Tibet can be explained by the Early Eocene Climate Optimum
- Global cooling and continental aridification likely drove paleobiogeographic change

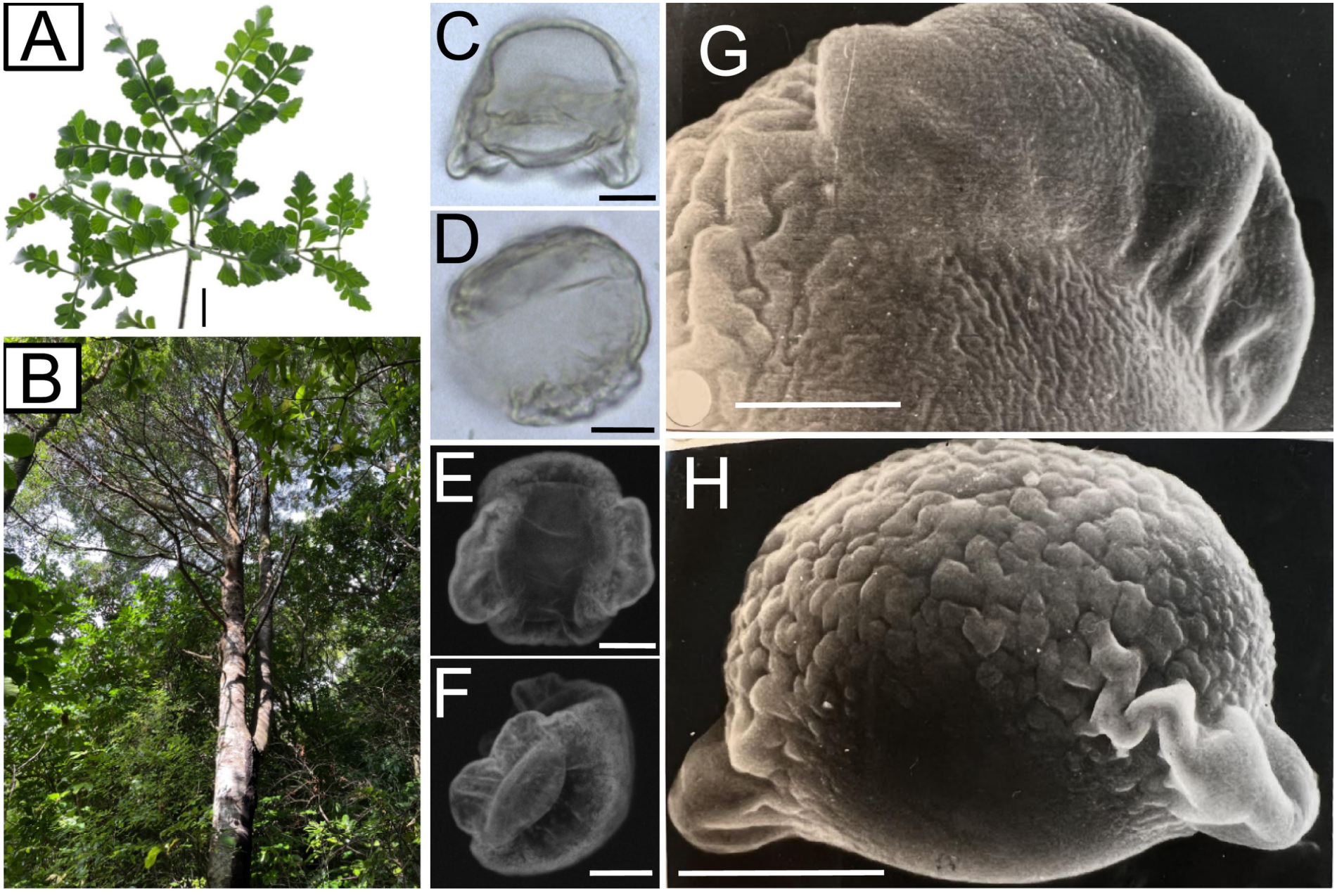

Figure 1

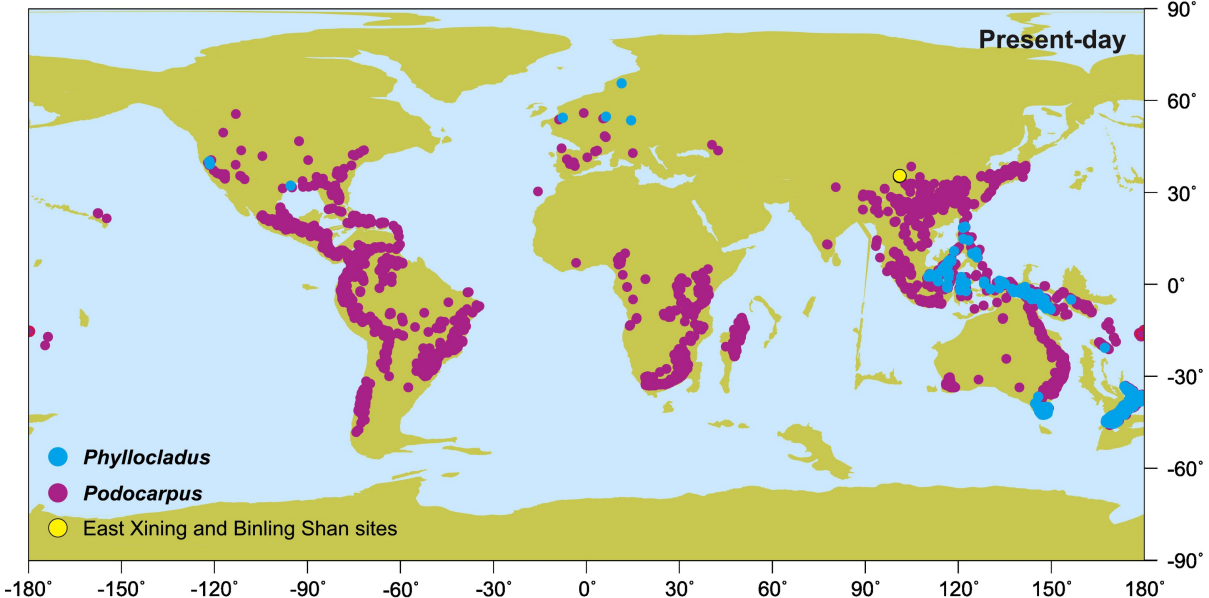
Present-day
Phyllocladus
Podocarpus
East Xining and Binling Shan sites
90˚
60˚
30˚
0˚
-30˚
-60˚
-90˚
-180˚
-150˚
-120˚
-90˚
-60˚
-30˚
0˚
30˚
60˚
90˚
120˚
150˚
180˚

Figure 2

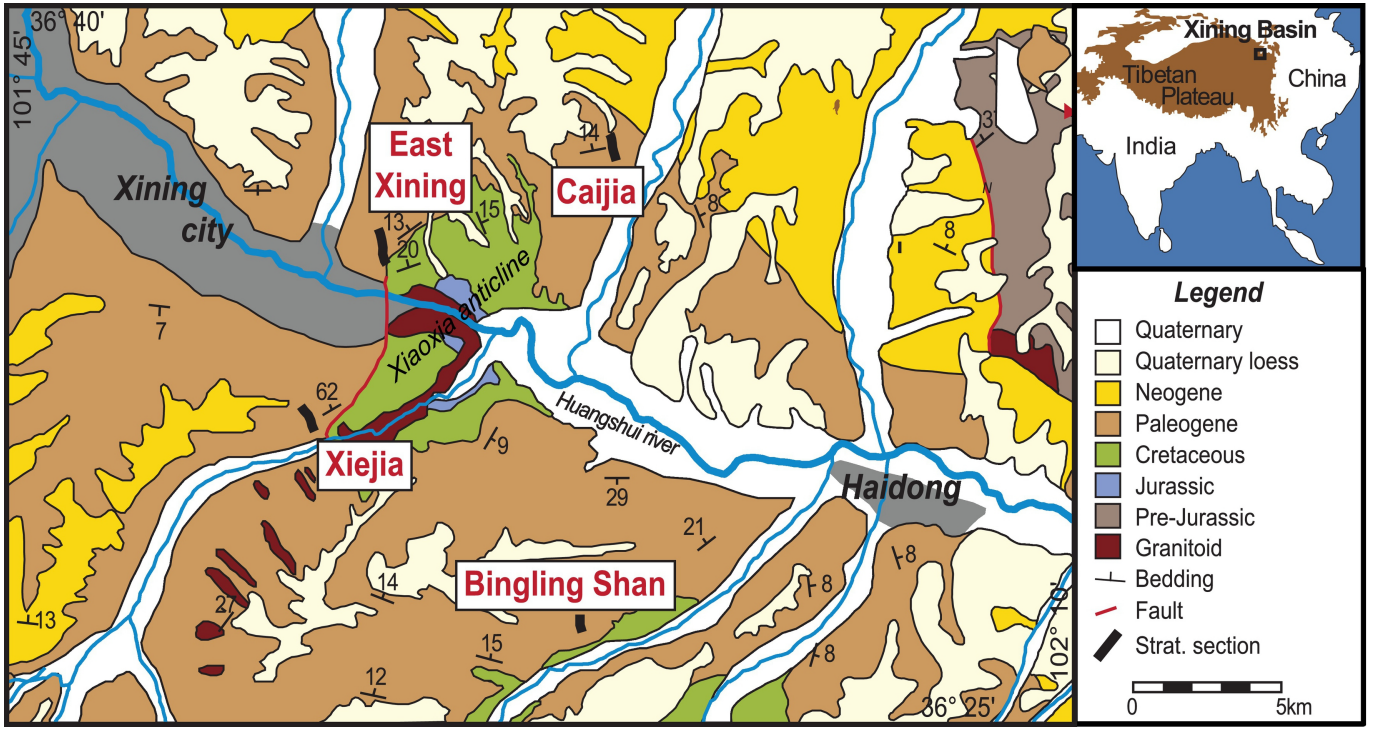
36° 40'
101° 45'
East Xining
Caijia
Xining city
Xiaoxia anticline
Huangshui river
Xiejia
Haidong
Bingling Shan
36° 25'
102° 10'
Xining Basin
Tibetan Plateau
China
India
Legend
Quaternary
Quaternary loess
Neogene
Paleogene
Cretaceous
Jurassic
Pre-Jurassic
Granitoid
Bedding
Fault
Strat. section
0
5km

Figure 3

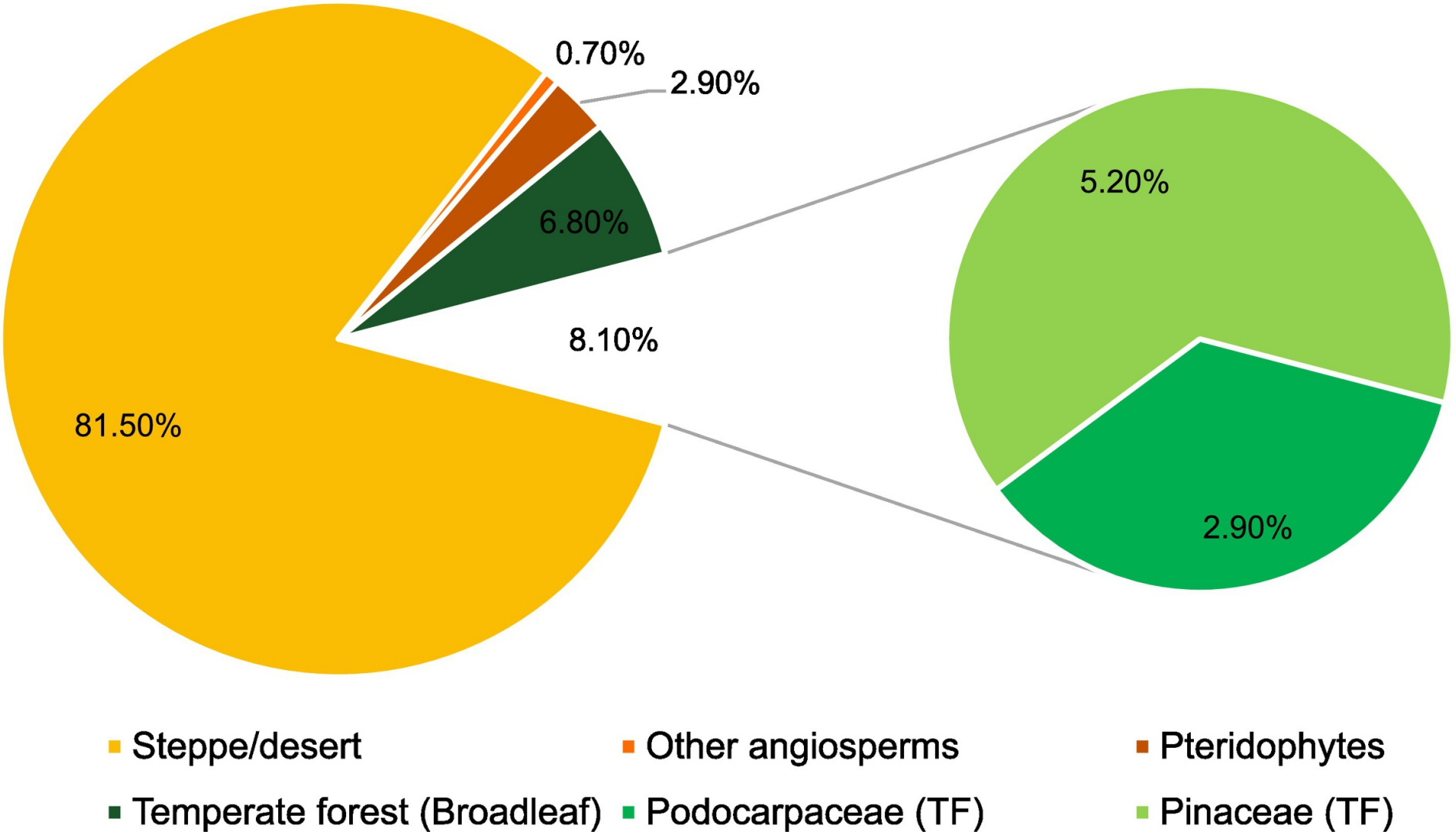
0.70%
2.90%
6.80%
8.10%
81.50%
5.20%
2.90%
Steppe/desert
Other angiosperms
Pteridophytes
Temperate forest (Broadleaf)
Podocarpaceae (TF)
Pinaceae (TF)

Figure 4

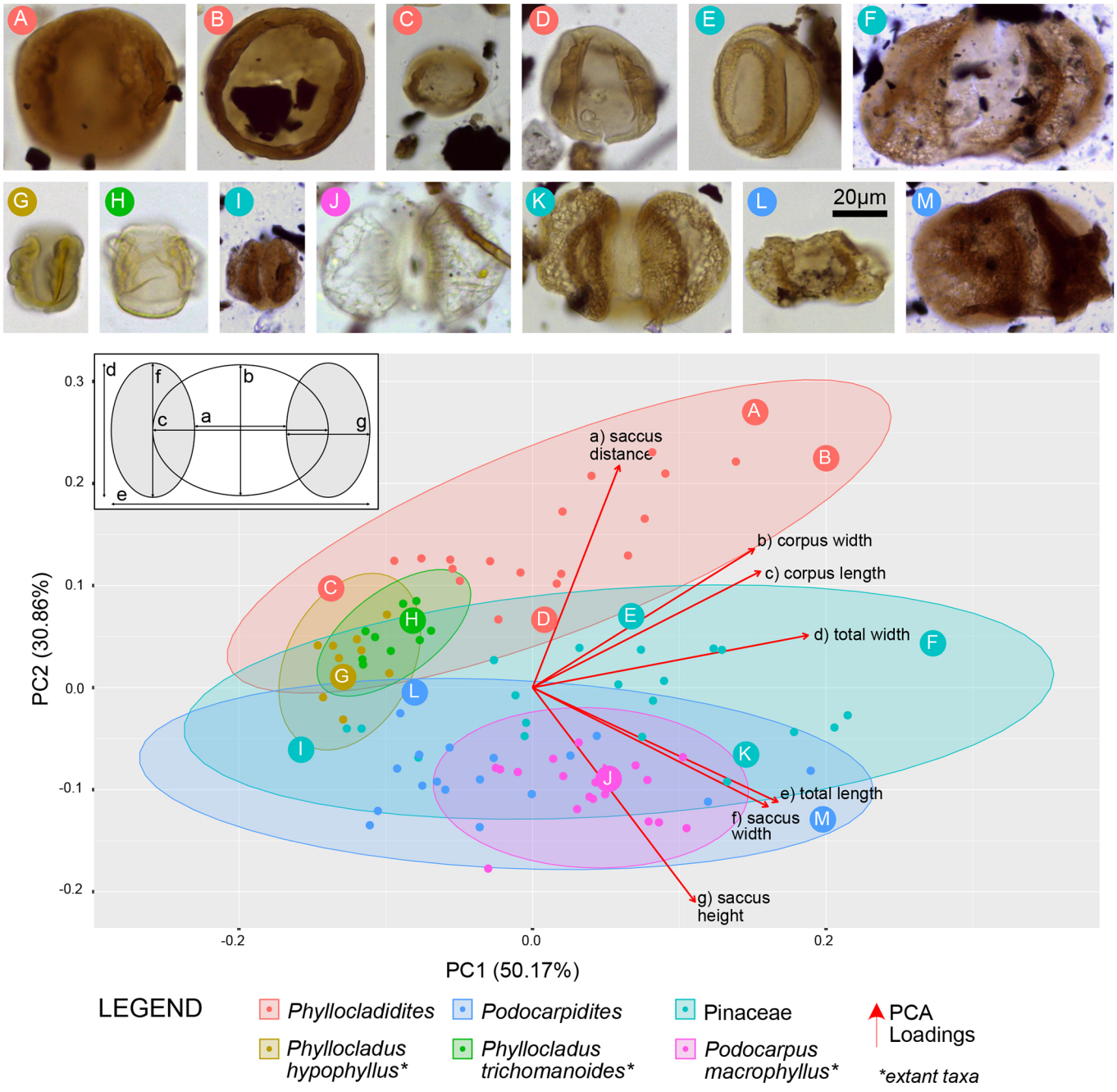
A
B
C
D
E
F
G
H
I
J
K
L
20µm
M
d
f
b
c
a
g
e
a) saccus distance
b) corpus width
c) corpus length
d) total width
e) total length
f) saccus width
g) saccus height
PC2 (30.86%)
PC1 (50.17%)
0.3
0.2
0.1
0.0
-0.1
-0.2
-0.2
0.0
0.2
LEGEND
Phyllocladidites
Podocarpidites
Pinaceae
PCA Loadings
Phyllocladus hypophyllus*
Phyllocladus trichomanoides*
Podocarpus macrophyllus*
*extant taxa

Figure 5

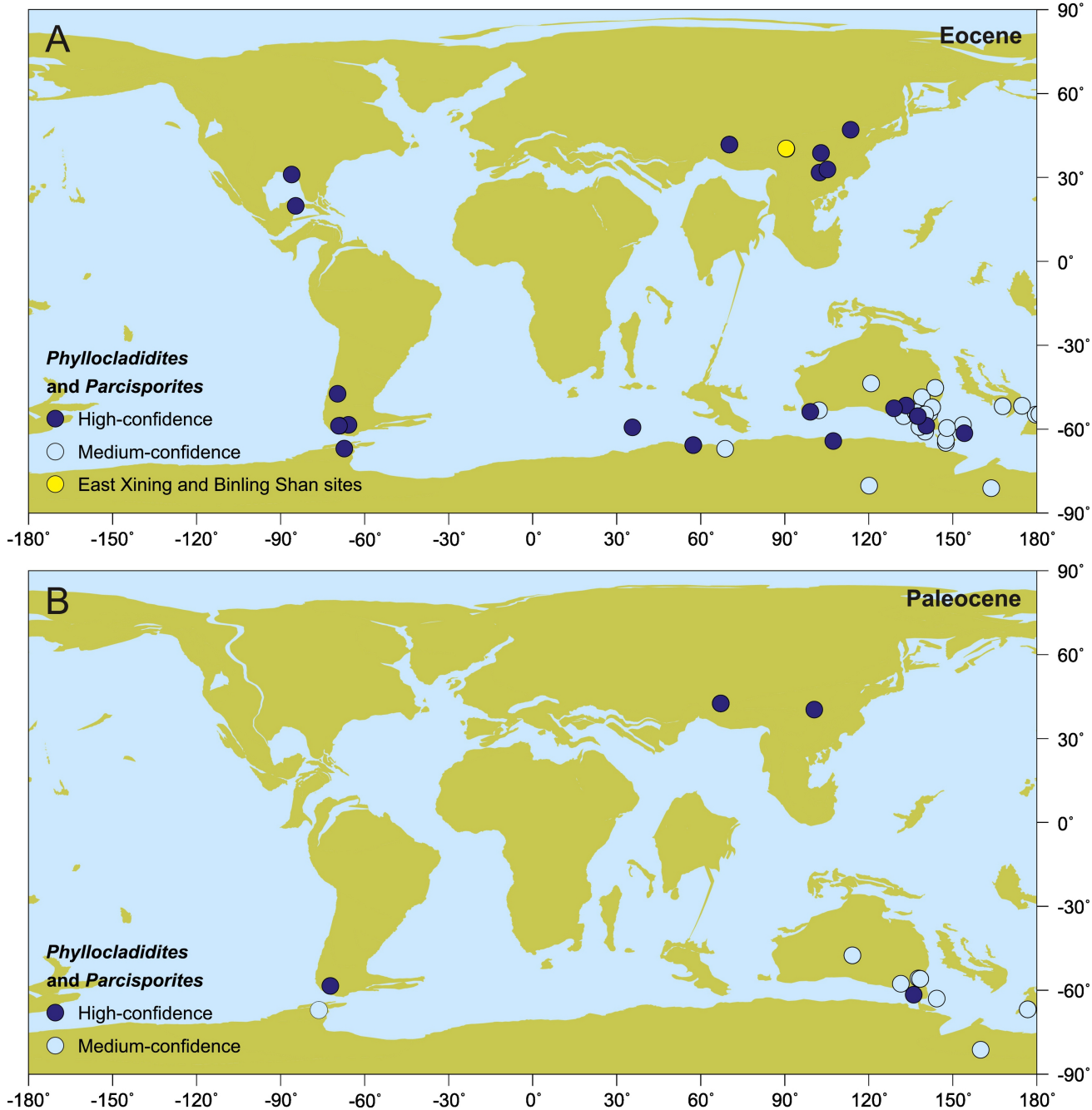
A
Eocene
Phyllocladidites
and Parcisporites
High-confidence
Medium-confidence
East Xining and Binling Shan sites
90˚
60˚
30˚
0˚
-30˚
-60˚
-90˚
-180˚
-150˚
-120˚
-90˚
-60˚
-30˚
0˚
30˚
60˚
90˚
120˚
150˚
180˚
B
Paleocene
Phyllocladidites
and Parcisporites
High-confidence
Medium-confidence
90˚
60˚
30˚
0˚
-30˚
-60˚
-90˚
-180˚
-150˚
-120˚
-90˚
-60˚
-30˚
0˚
30˚
60˚
90˚
120˚
150˚
180˚

Figure 6

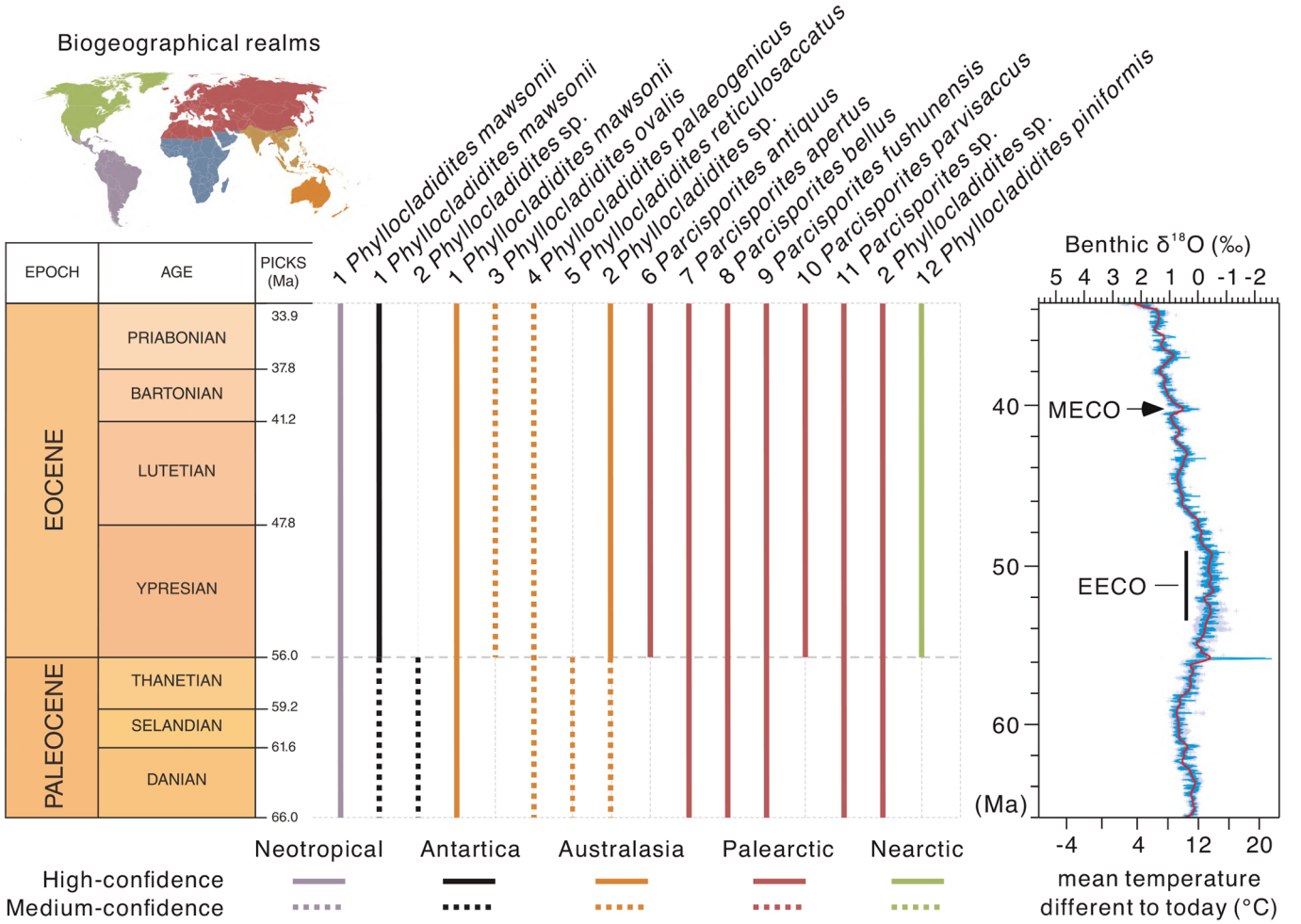
Biogeographical realms
1 Phyllocladidites mawsonii
1 Phyllocladidites mawsonii
2 Phyllocladidites sp.
1 Phyllocladidites mawsonii
3 Phyllocladidites mawsonii
4 Phyllocladidites ovalis
5 Phyllocladidites palaeogenicus
2 Phyllocladidites reticulosaccatus
6 Parcisporites sp.
7 Parcisporites antiquus
8 Parcisporites apertus
9 Parcisporites bellus
10 Parcisporites fushunensis
11 Parcisporites parvisaccus
2 Phyllocladidites sp.
12 Phyllocladidites piniformis
EPOCH
AGE
PICKS (Ma)
EOCENE
PRIABONIAN
BARTONIAN
LUTETIAN
YPRESIAN
PALEOCENE
THANETIAN
SELANDIAN
DANIAN
33.9
37.8
41.2
47.8
56.0
59.2
61.6
66.0
Neotropical
Antartica
Australasia
Palearctic
Nearctic
High-confidence
Medium-confidence
Benthic δ18O (‰)
5 4 3 2 1 0 -1 -2
40
50
60
(Ma)
MECO
EECO
-4
4
12
20
mean temperature different to today (°C)

Figure 7

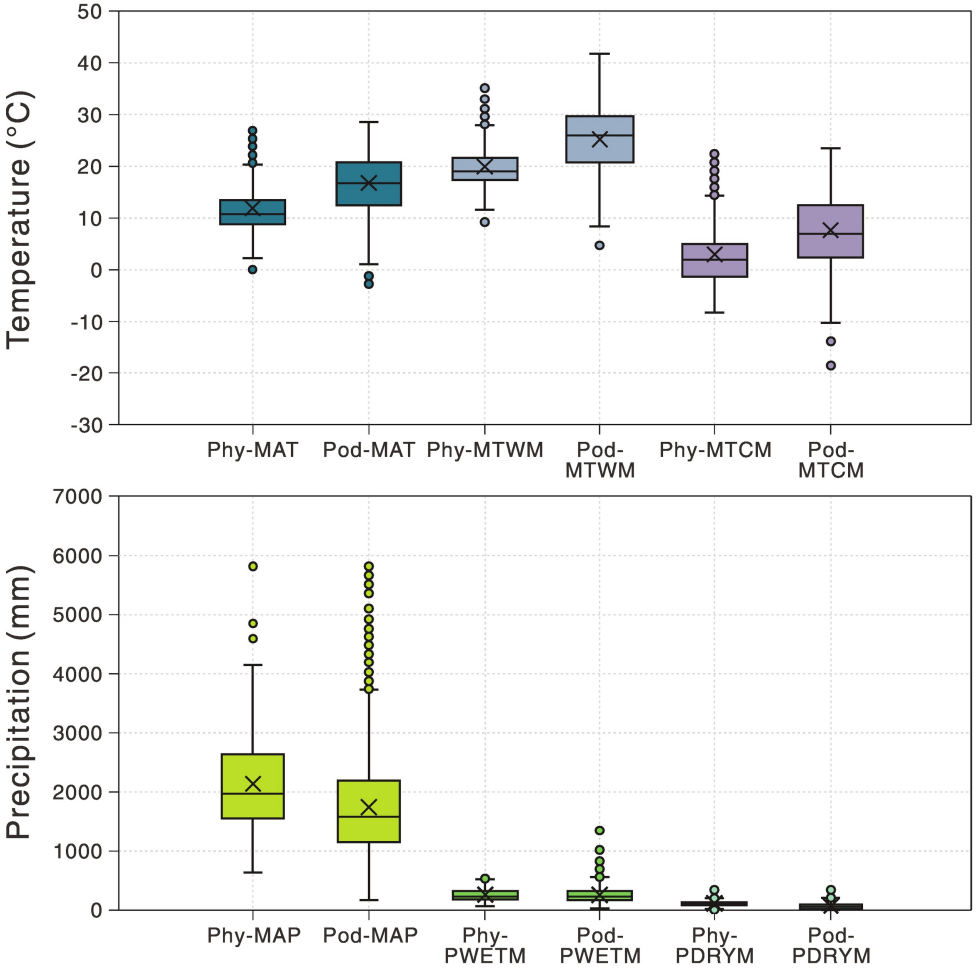
Temperature (°C)
50
40
30
20
10
0
-10
-20
-30
Phy-MAT
Pod-MAT
Phy-MTWM
Pod-MTWM
Phy-MTCM
Pod-MTCM
Precipitation (mm)
7000
6000
5000
4000
3000
2000
1000
0
Phy-MAP
Pod-MAP
Phy-PWETM
Pod-PWETM
Phy-PDRYM
Pod-PDRYM

Figure 8